(9) Photocatalysis
(PEC(Photoelectrochemical) cell)

1. Overview for photoelectrochemistry: water splitting

PECs are solar cells that produce electrical energy or H_2 in a process similar to the electrolysis of H_2O.

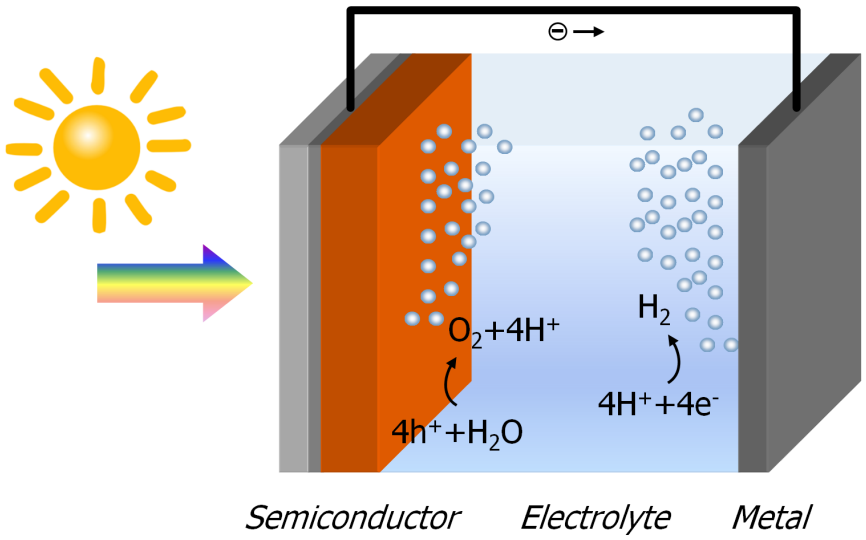

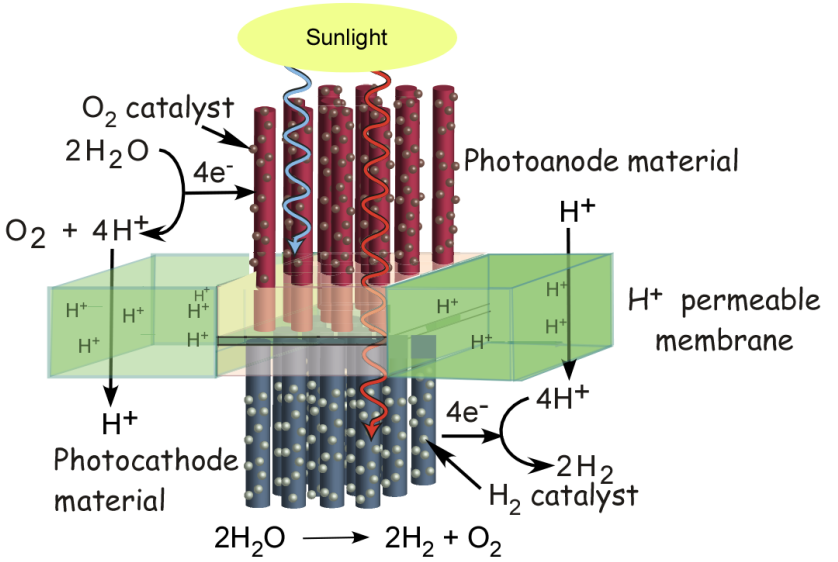

JCAP
JOINT CENTER FOR ARTIFICIAL PHOTOSYNTHESIS

Fundamental challenges for photovoltaic (PV) cells
: very low conversion efficiency

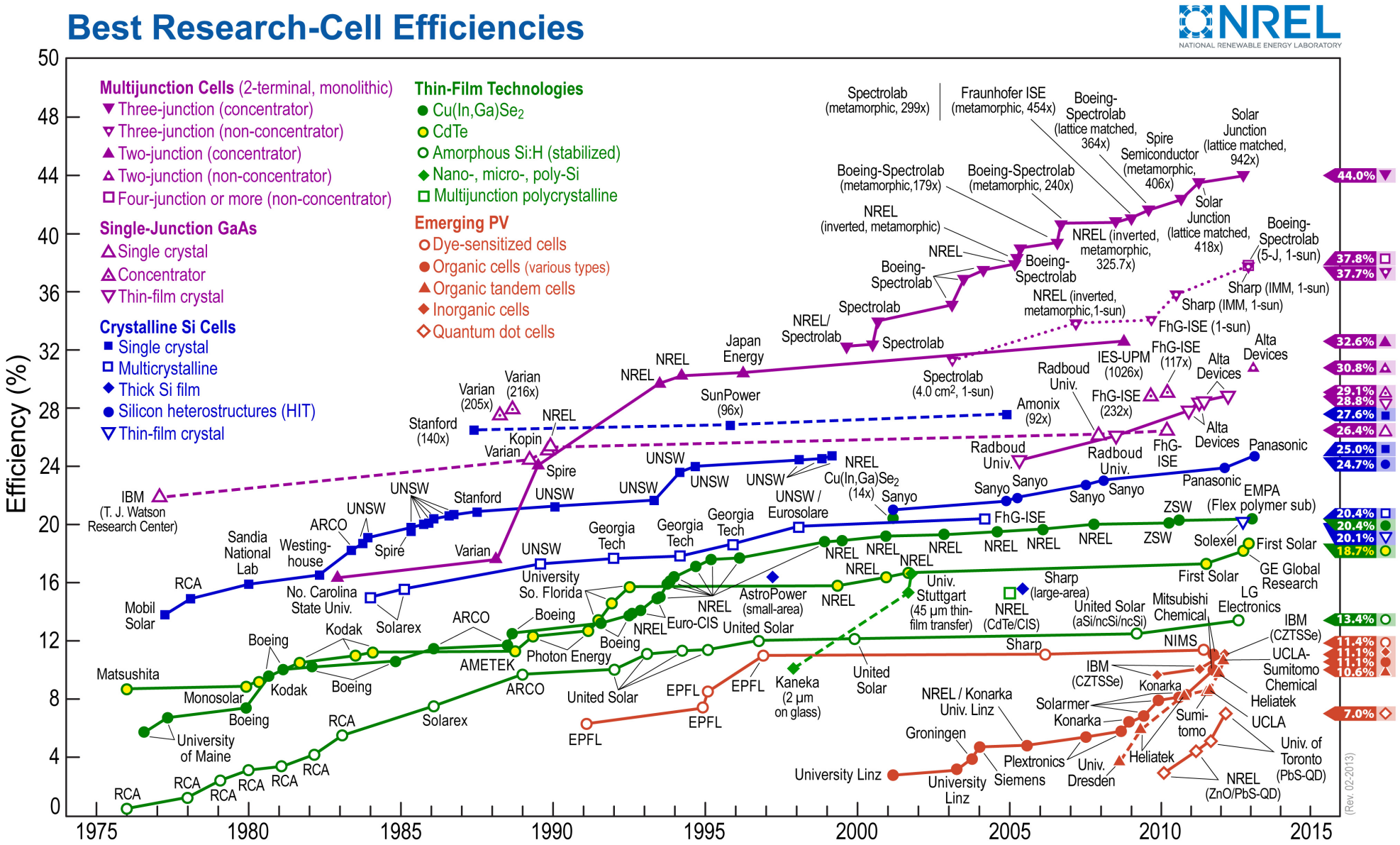

https://www.greentechmedia.com/content/images/articles/NREL-PV-eff-3-13.jpg

• Requirements and trade-offs for photoelectrode

- ○ Good (visible) light absorption
- ○ Efficient charge transport in the semiconductor
- ○ High chemical stability in the dark and under illumination and in sol'n
- ○ Negligible photocorrosion (with increasing E_g semiconductor)
- ○ Low cost
- ○ Band edge positions that straddle the water reduction and oxidation potential
- ○ Low overpotentials for reduction/oxidation of water

• Minimum/Maximum bandgap (E_g) for photoelectrode

1.23 eV	+	0.3~0.4 eV	+	0.4~0.6 eV	≤	**1.9 eV**
Thermodynamic potential for water splitting		Thermodynamic loss (for semiconductor)		Overpotential (for OER)		Absorption onset at 650 nm (wavelength)

Not over **3.1 eV**: below 400 nm of wavelength the intensity of sunlight drops rapidly.

• Solar energy efficiency of water splitting

$$\frac{Chemical\ potential}{Electrolysis\ potential} = \frac{1.23}{1.9} = 65\%$$

- ○ Coupling to a 12% PV (photovoltaic) array gives a solar-to-hydrogen efficiency of 0.12 x 0.65 = **7.8%**

Bandgap Considerations

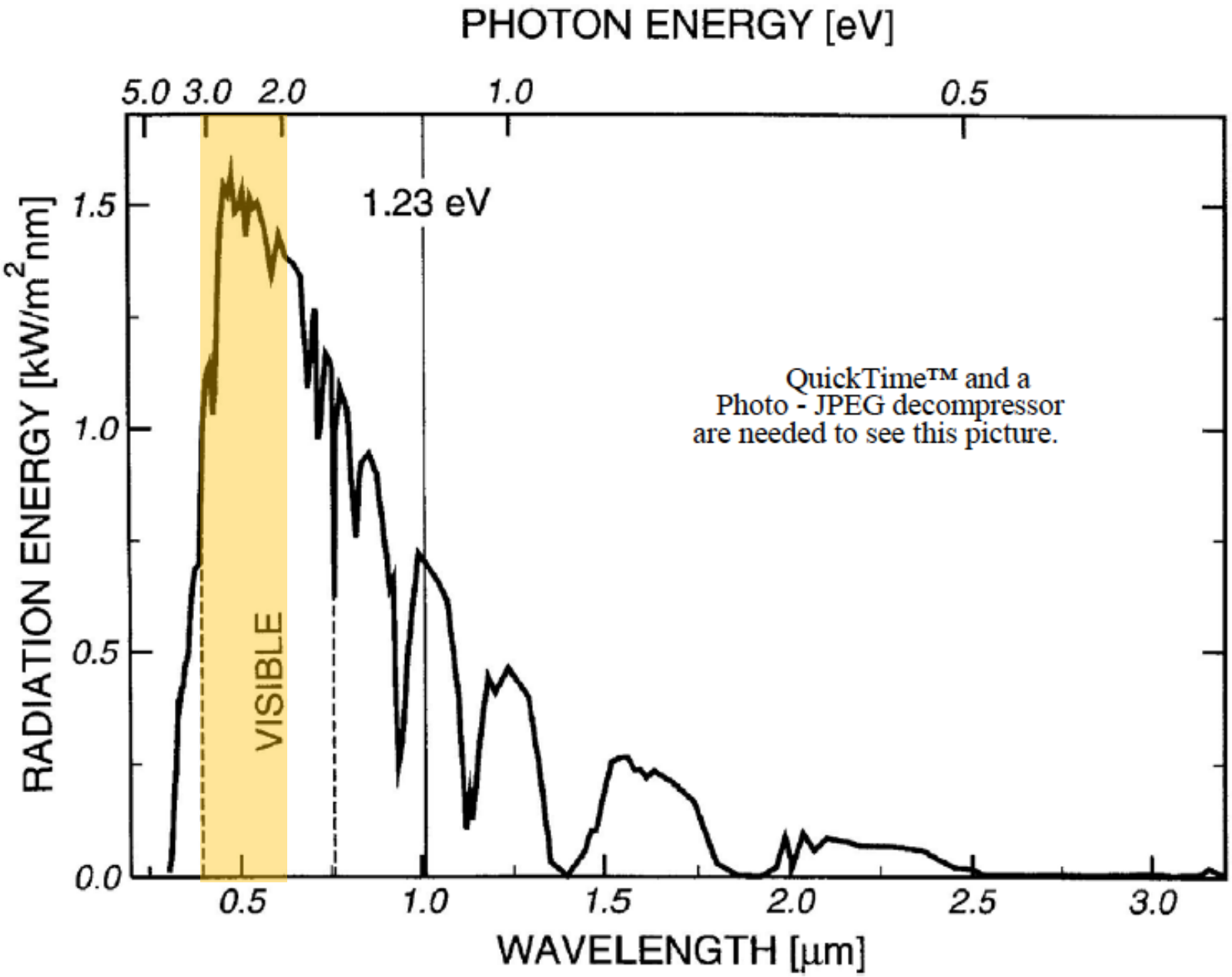

2. Semiconductors for photoelectrode

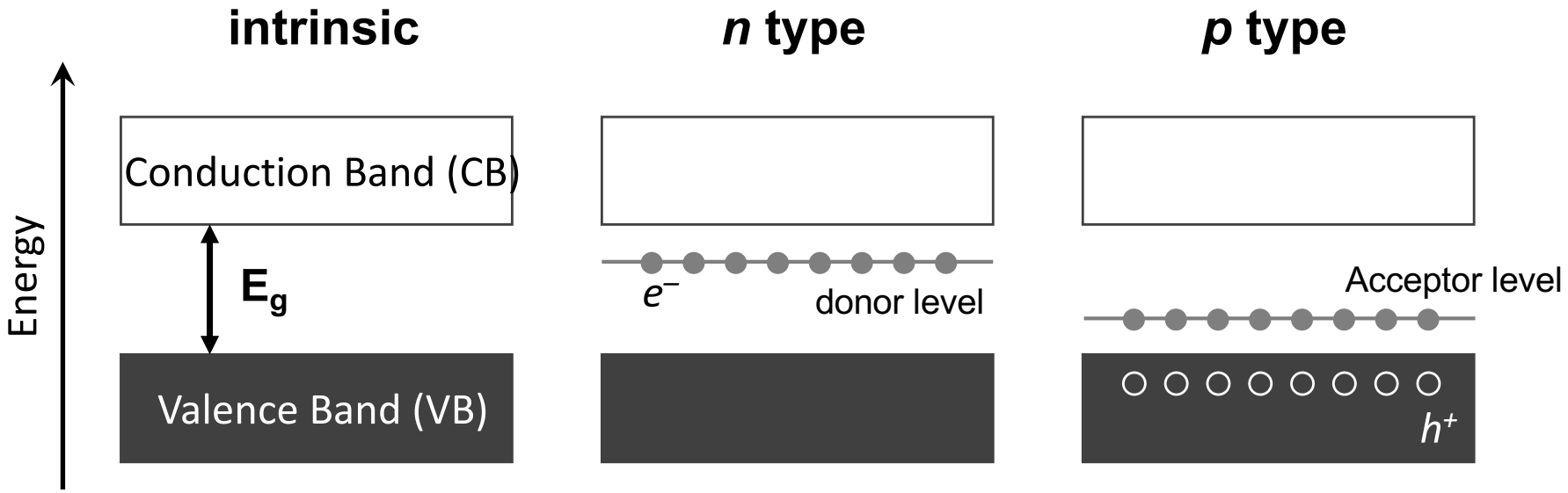

Majority carrier: e^-
Minority carrier: h^+

Majority carrier: h^+
Minority carrier: e^-

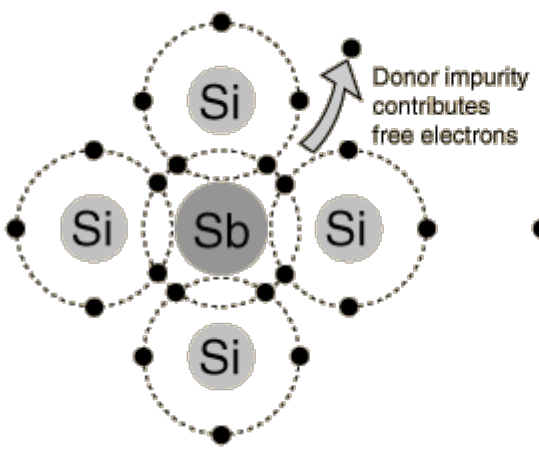

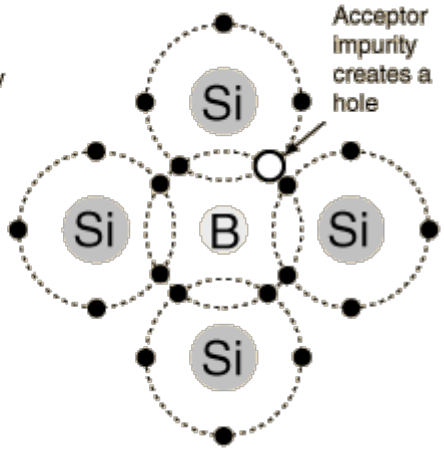

3. Photochemical reaction process

(1) Photon absorption

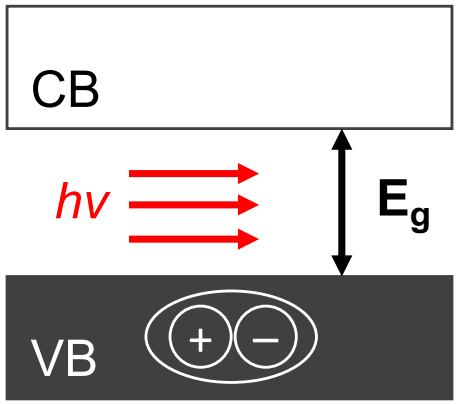

exciton

Generation of e^- and h^+ with sufficient potentials

(2) Charge separation

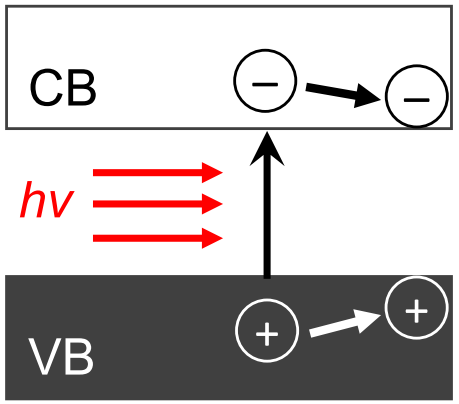

And migration to surface reaction sites

(3) Electrochemical rxn

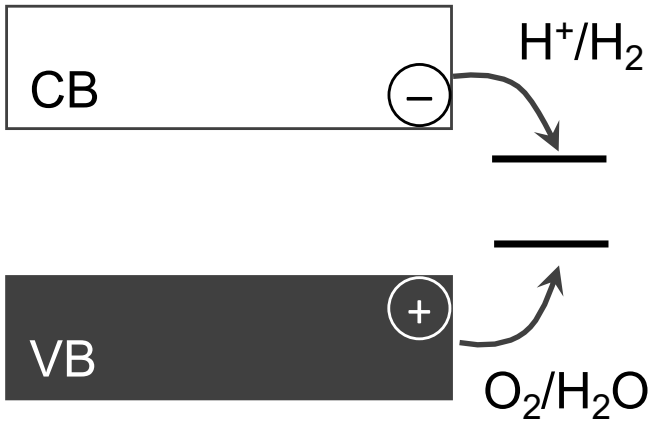

Construction of surface rxn sites for H_2/O_2 evolution

(4) Recombination

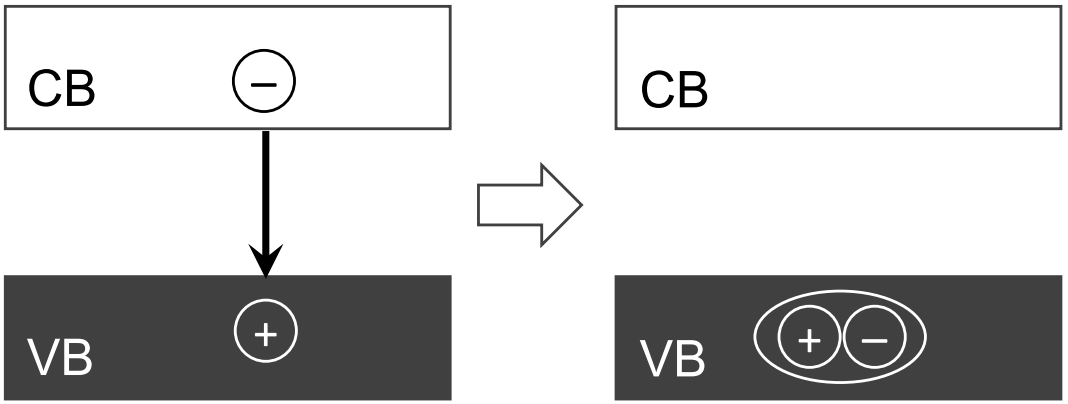

No further rxn

3-1. bandgap

(1) Photon absorption

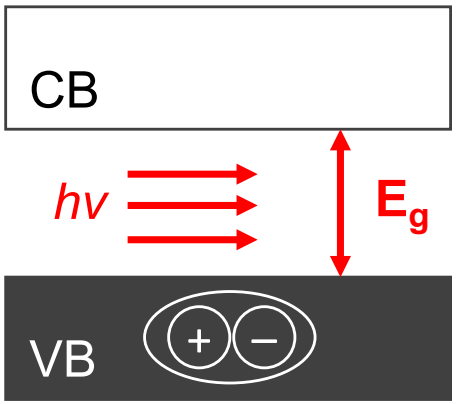

exciton

Generation of e^- and h^+ with sufficient potentials

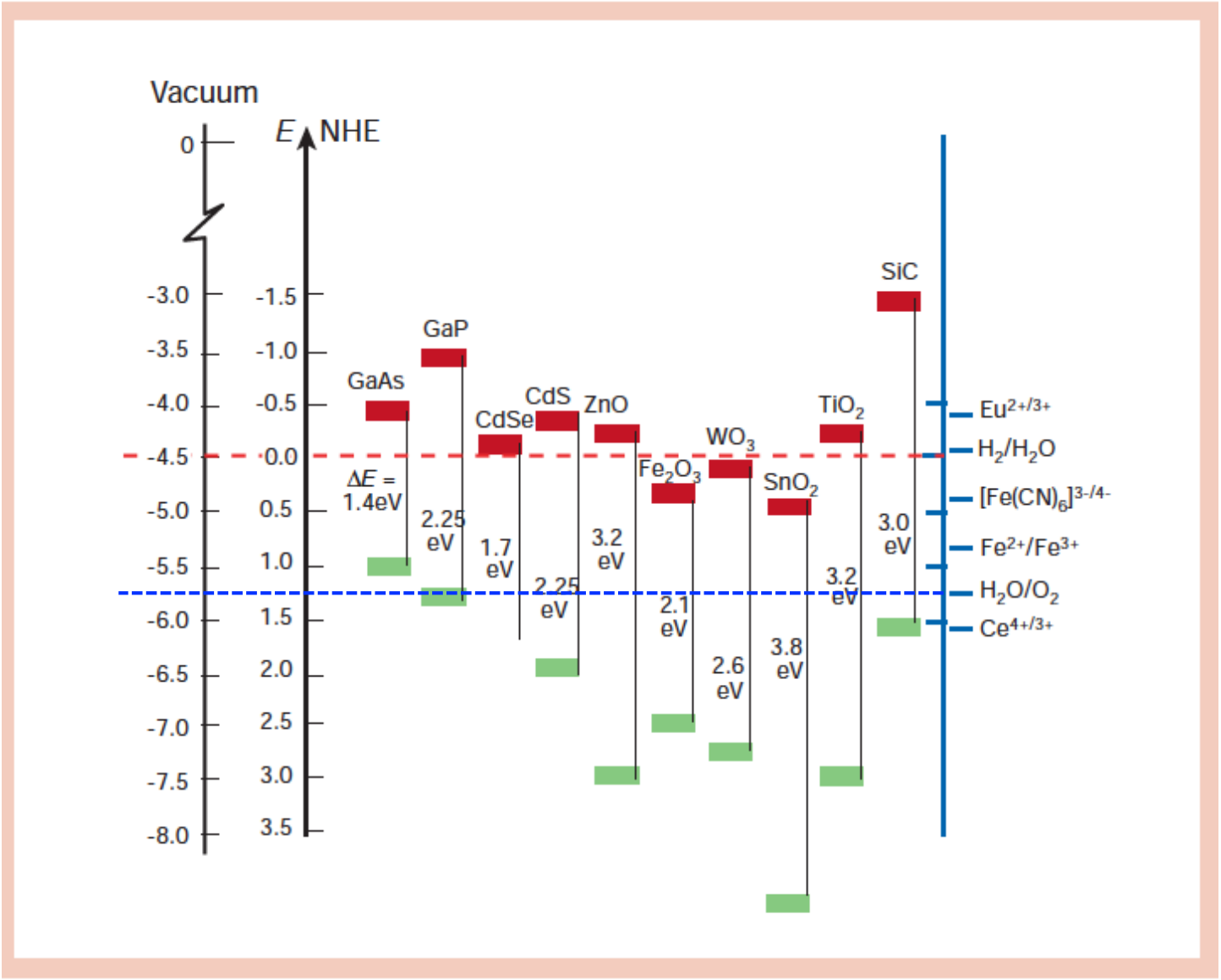

M. Gratzel, *Nature* **2011**, *414*, 338-344.

3-2. Band edge position (quasi-Fermi level)

(3) Electrochemical rxn

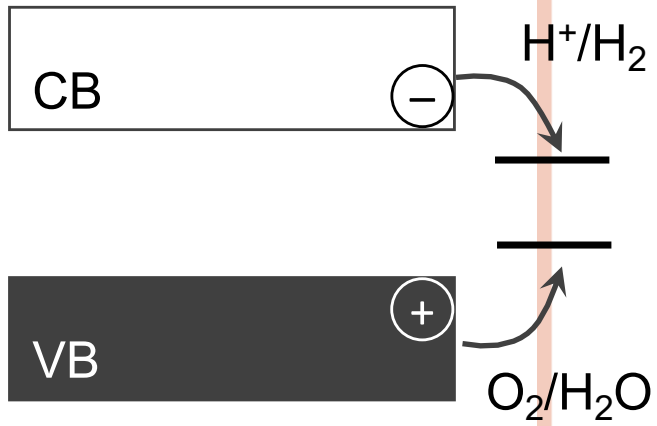

Construction of surface rxn sites for H_2/O_2 evolution

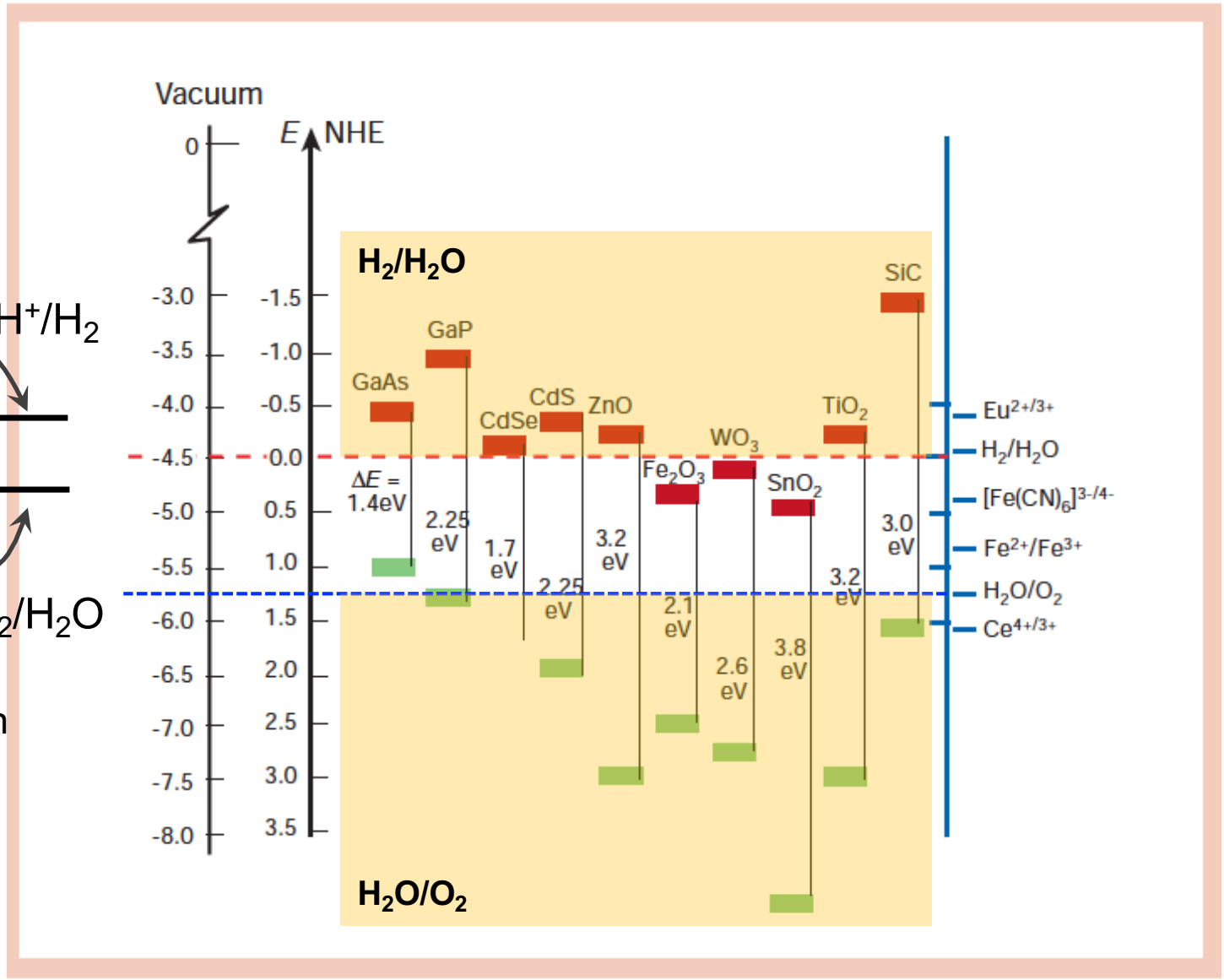

M. Gratzel, *Nature* **2011**, *414*, 338-344.

3-3. Direct and indirect bandgap

Direct bandgap

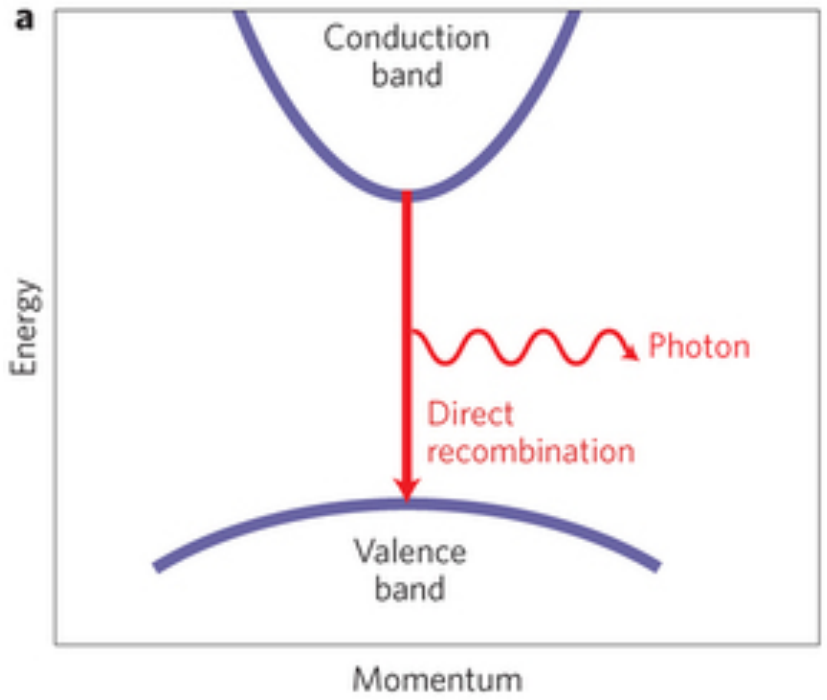

- Excellent light absorption
- Thin film solar cell (< 1 μm, CdTe, CIGS..)

Indirect bandgap

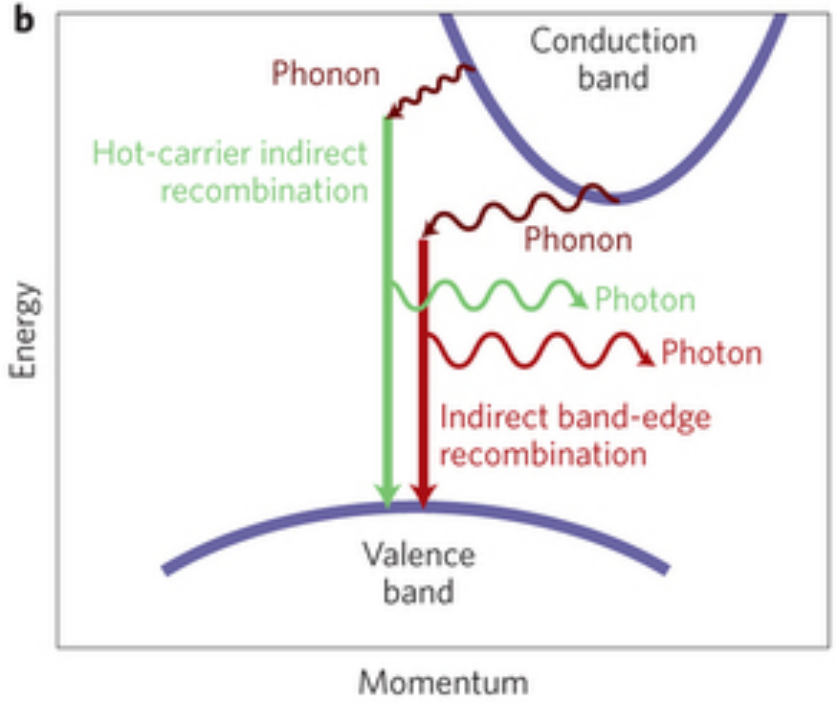

- Requiring a change in crystal momentum
- Poor light absorption
- Thick film solar cell (Si)
- Radiative recombination is slower.

- The recombination occurring at boundaries and defects.

*CIGS: copper indium gallium selenide

- **Absorption coefficient, α**

$$\alpha = \frac{A(h\nu - E_g)^m}{h\nu}$$

A: constant
m : $^1/_2$ for a direct bandgap and 2 for an indirect bandgap

- **Tauc plot ➔ Measurement of E_g for semiconductor**

Extrapolation of a plot of $(\alpha h\nu)^{1/2}$ vs. $h\nu$: the indirect bandgap
a plot of $(\alpha h\nu)^2$ vs. $h\nu$: the direct bandgap

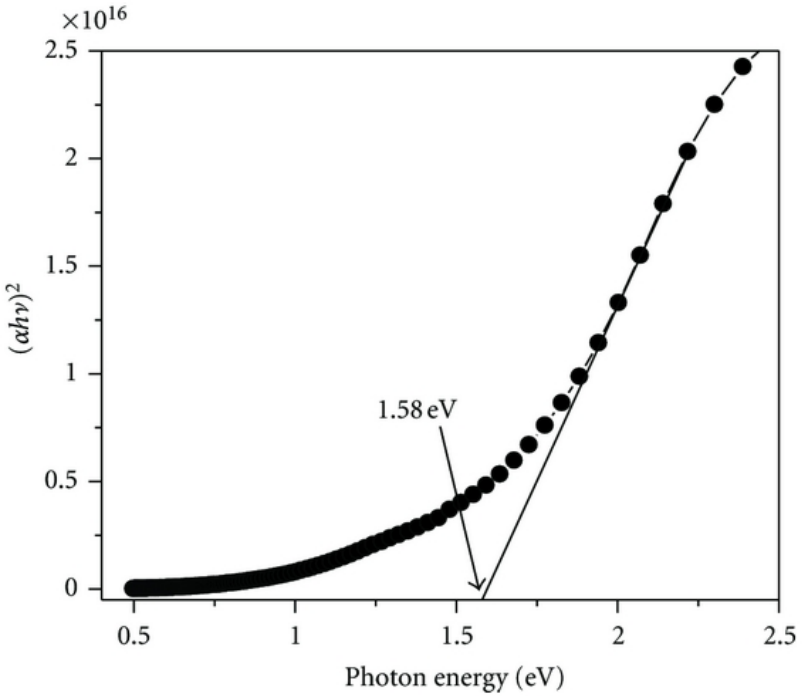

3-4. Configuration of PEC cell

(1) One body

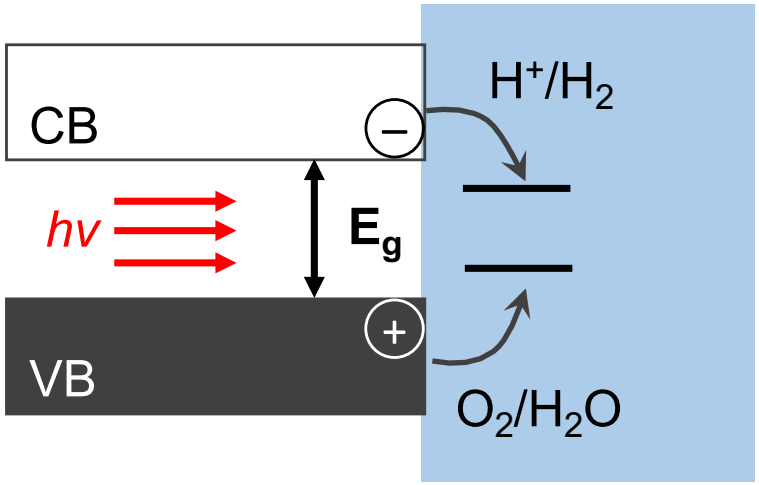

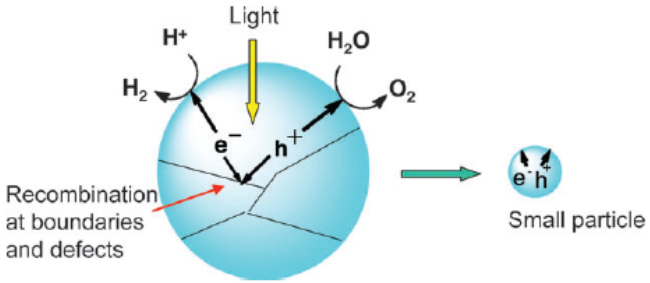

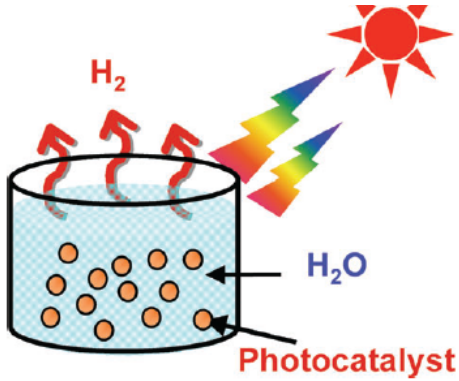

(2) Photoanode

Higher efficiency

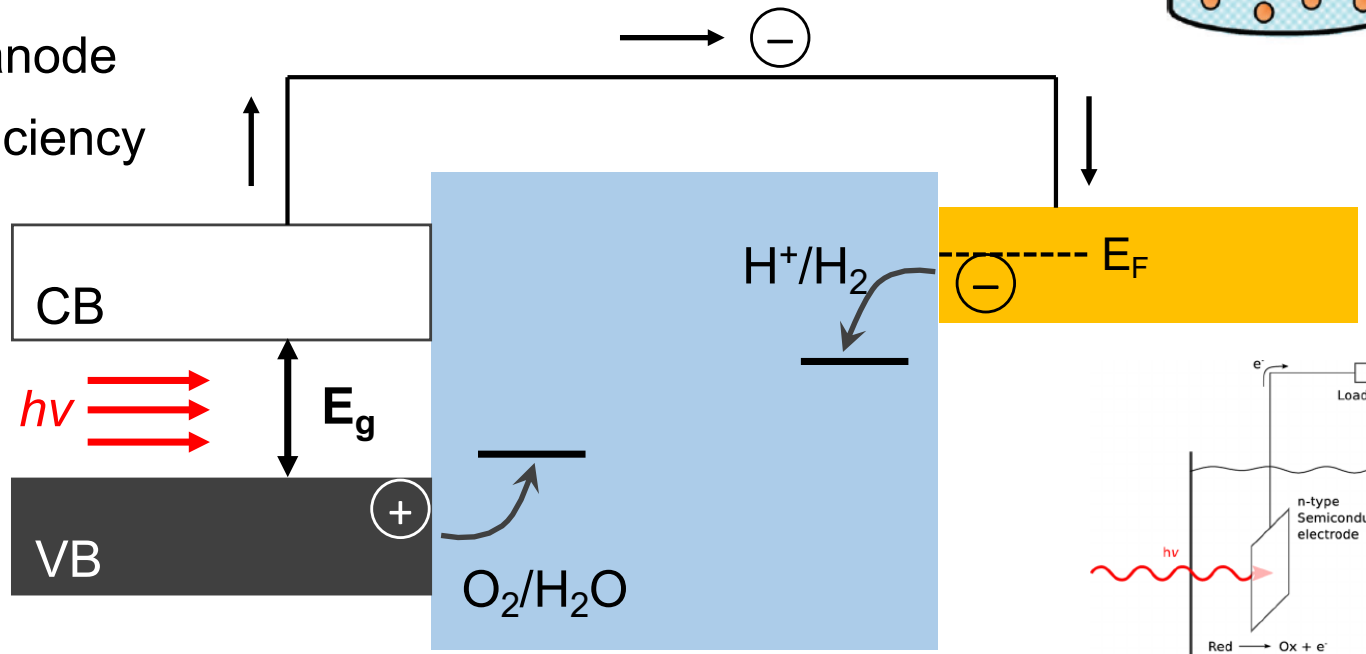

Semiconductor (WE) electrolysis Metal (CE)

Chem. Soc. Rev. **2009**, *38*, 253-278.

4. Semiconductor/electrolyte interface (for *n* type semiconductor)

Schottky contact
(semiconductor/metal contact)

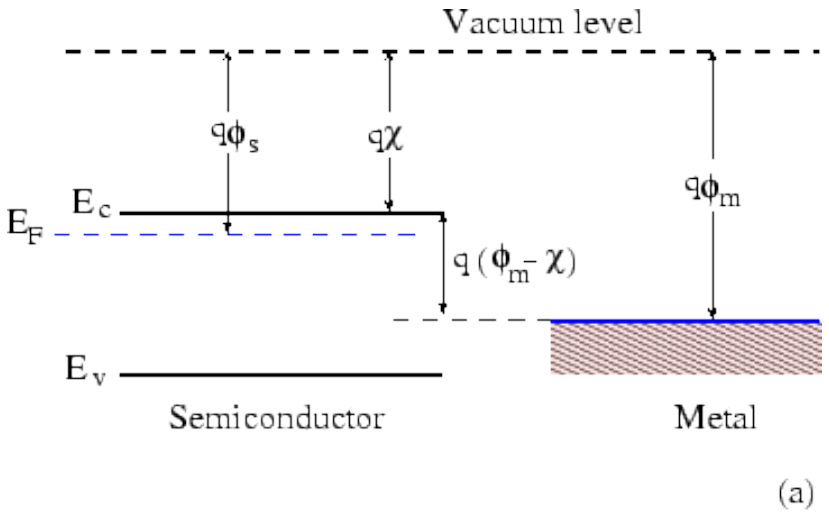

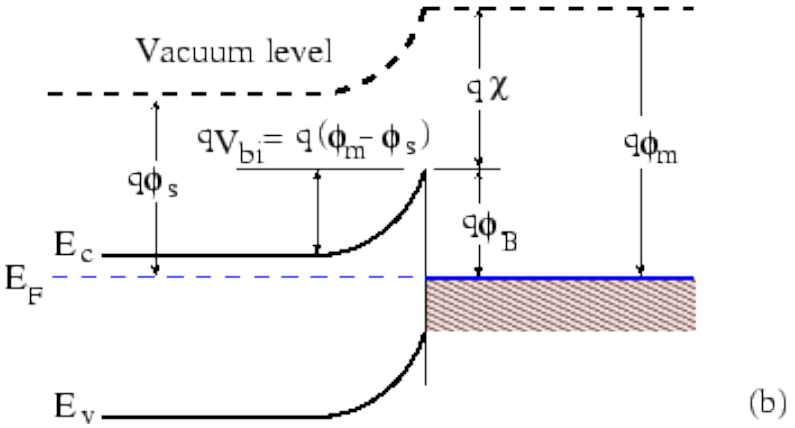

Semiconductor/electrolyte contact

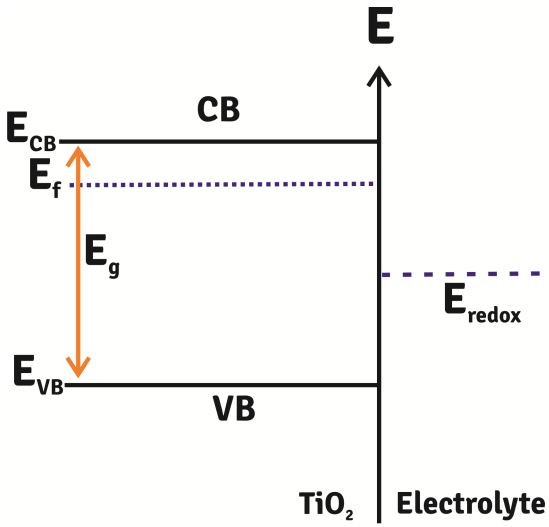

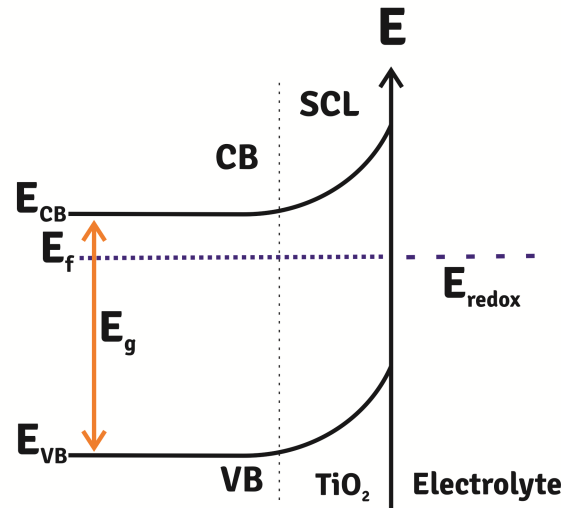

Becoming equilibrium

4-1. Space charge : *excess electric charge* present in a region of space (at the semiconductor/liquid electrolyte junction (SCLJ))

- The physical origin of surface state: structural defects (dangling bonds, vacancies, etc) or chemisorbed species from an electrolyte sol'n.

- When a metal oxide is exposed to air, water molecules from the air can dissociatively adsorb at its surface, resulting in –OH surface termination.

- Surface hydroxylation
  - pH dependence for electrolyte solution
  - BrØnsted acidity of the semiconductor surface

$$M\text{–}OH \rightleftarrows MO^- + H^+_{aq}$$
$$M\text{–}OH + H^+_{aq} \rightleftarrows M\text{–}OH_2^+$$

- These –OH groups form electronic surface states within the E_g of the semiconductor.

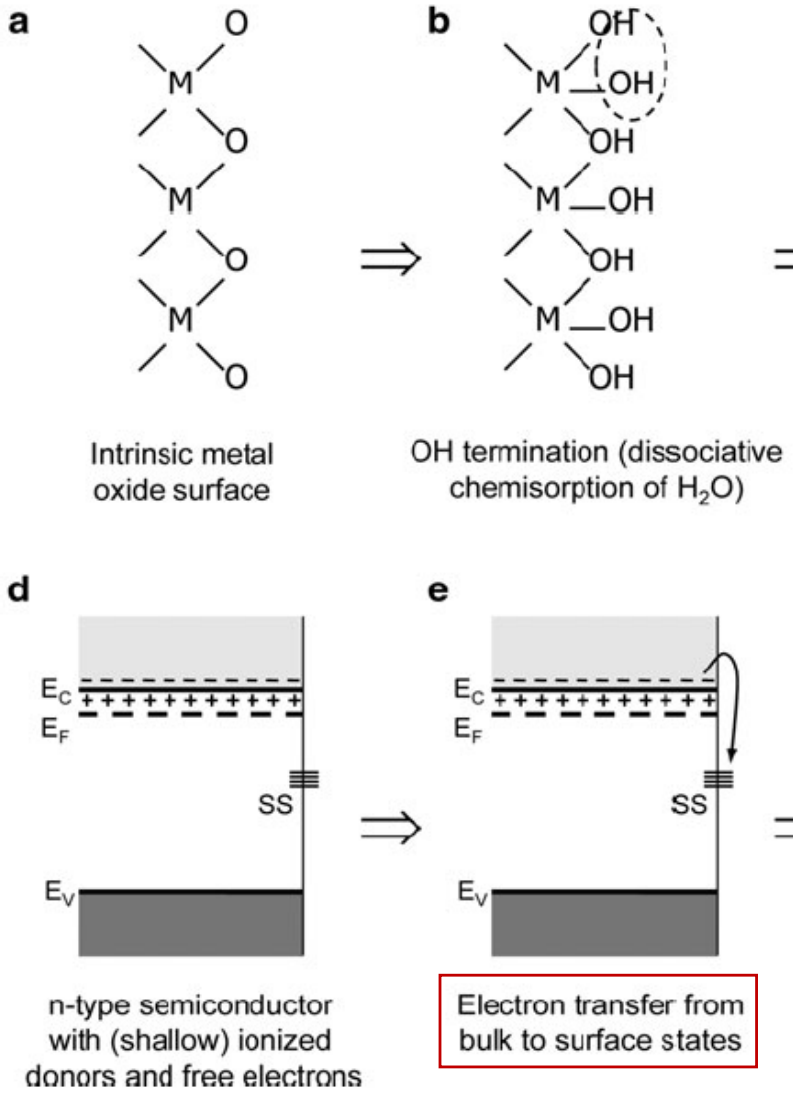

R. Van de Krol and M. Gratzel, *Photoelectrochemical Hydrogen Production*

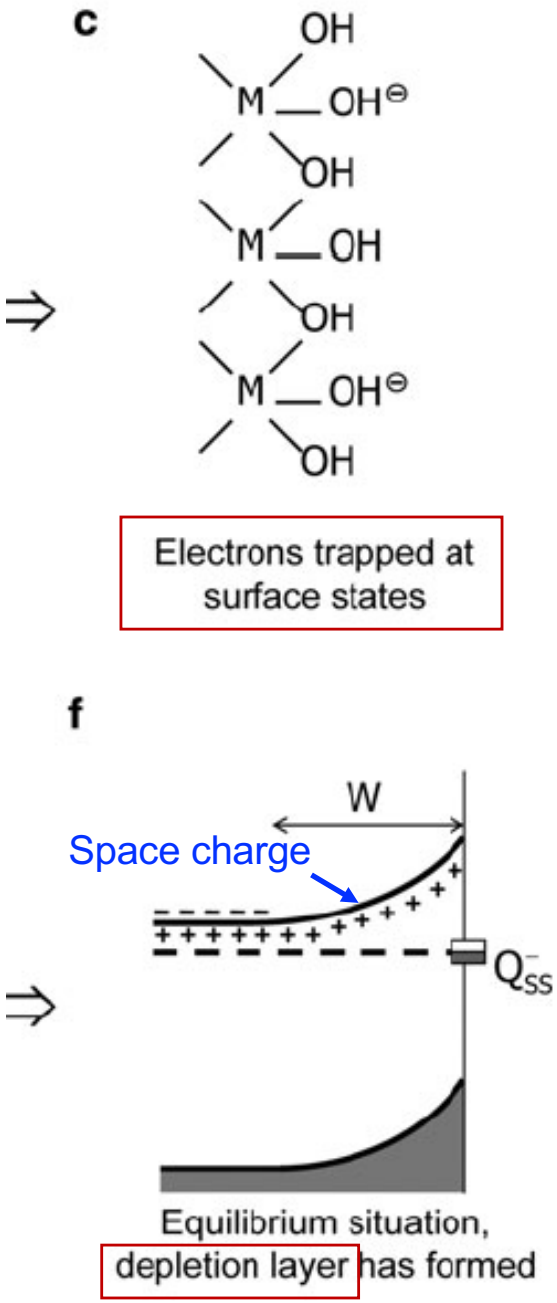

○ An electric field forms, and the charge transfer from bulk to surface will continue until the potential barrier becomes too large for bulk electrons to cross. At this point, a dynamic equilibrium establishes at which no net e^- transport takes place.

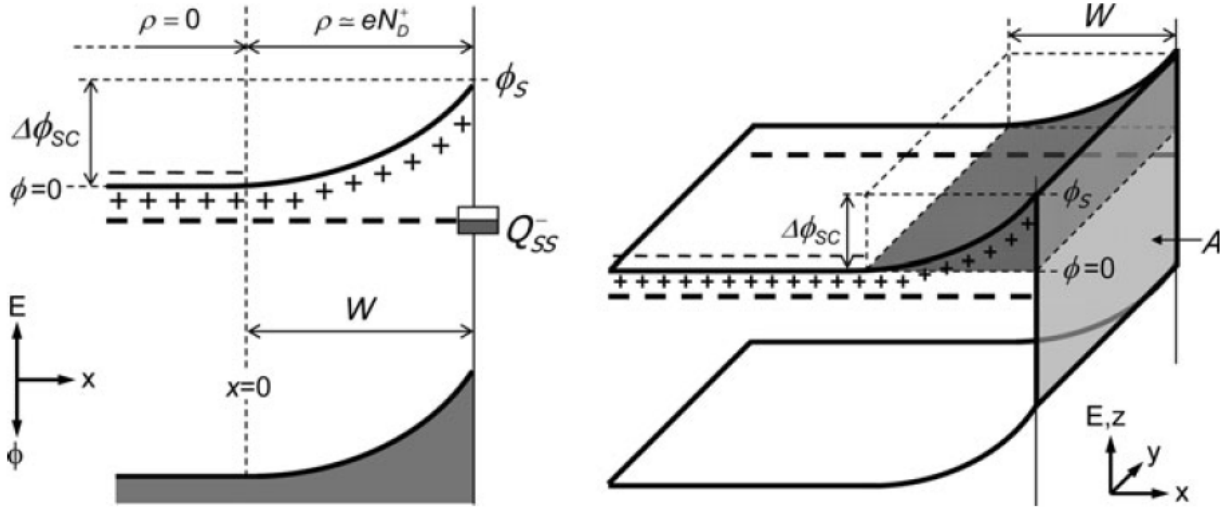

Fig. 2.12 Illustration of band bending at the surface of a n-type semiconductor in depletion. The "+" markers just below the conduction band represent the ionized donor species, whereas the "−" markers just above the conduction band level represent the free electrons. The potential in the bulk of the semiconductor is chosen as zero

○ The potential distribution and width of space charge depend on the amount of charges transferred to the surface and the density of shallow donors in the material.

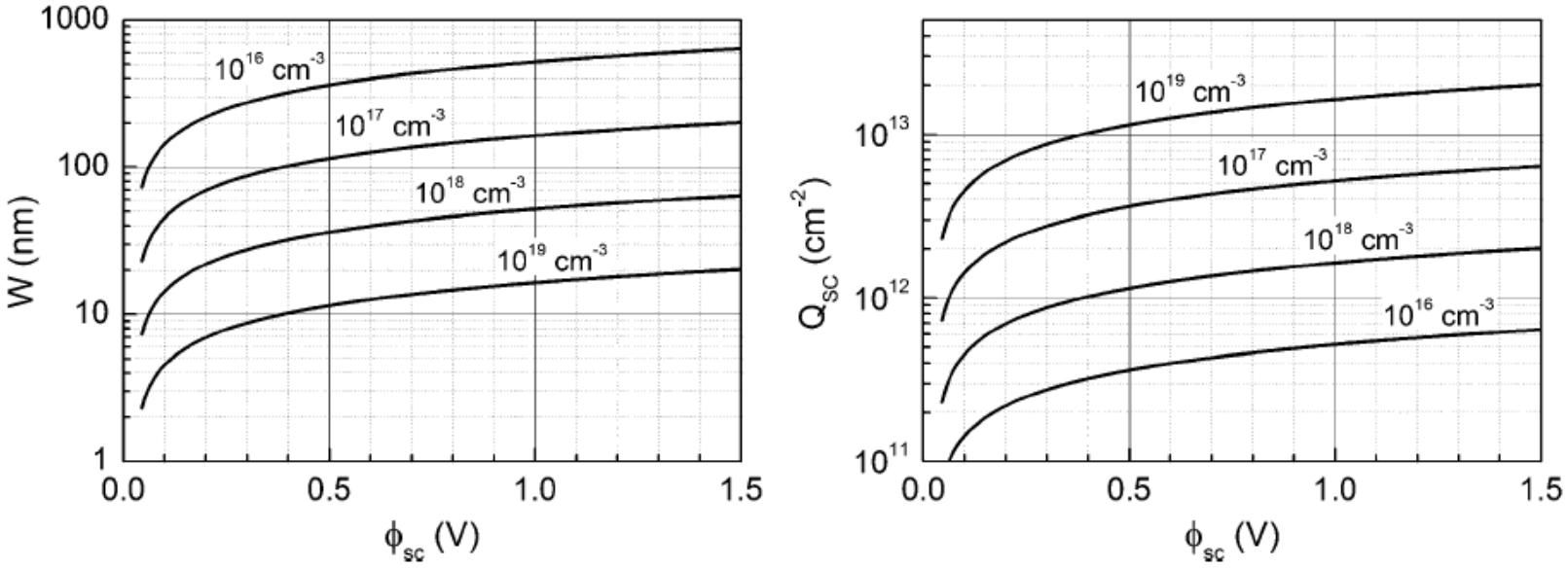

Fig. 2.13 *Left*: Depletion layer width as a function of potential drop across the space charge (ϕ_{SC}) and (shallow) dopant density. *Right*: Corresponding amount of adsorbed surface charges needed to compensate the charges in the depletion layer. The data are calculated for α-Fe_2O_3 assuming a static dielectric constant of 25 [39, 40]

○ Upon irradiation, photogenerated carriers are separated by the space-charge field and the minority carriers travel to the SCLJ to perform on O_2 evolution.

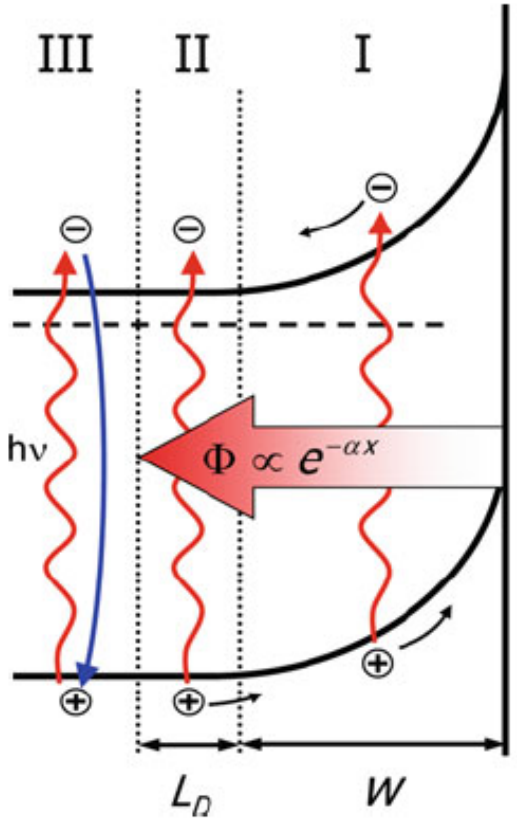

Region I:
- Absorption
- Charge separation
- Field-assisted transport (drift)

Region II:
- Absorption
- Transport by diffusion
- Holes are able to reach region I before recombining

Region III:
- Absorption + recombination

Optimal film thickness: $d \approx \alpha^{-1} \approx W + L_D$

Fig. 2.23 Absorption regions in a semiconducting photoanode. The intensity of the light (Φ) decreases exponentially with distance from the surface (Lambert-Beer law). All charge carriers generated within a distance $L_D + W$ from the surface contribute to the photocurrent (regions I and II), whereas all carriers generated in region III recombine

R. Van de Krol and M. Gratzel, *Photoelectrochemical Hydrogen Production*

- The charges at the surface: e^- trapped in surface states + adsorbed ions
- The counter charge: ionized donors in the semiconductor + an accumulation of oppositely charged ions in the electrolyte sol'n.
- V_H depends on the pH of the sol'n.

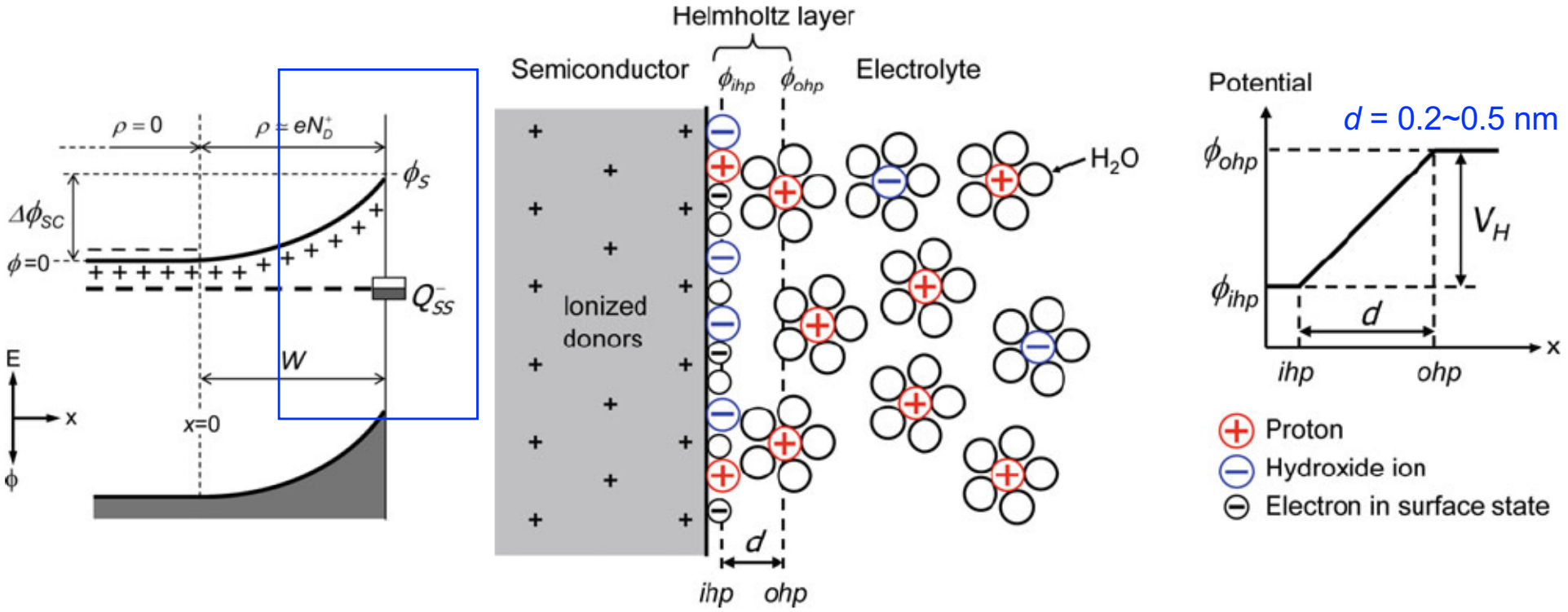

Fig. 2.15 Schematic model of the semiconductor/electrolyte interface and the Helmholtz layer. The inner Helmholtz plane (*ihp*) consists of H^+ and OH^- ions that are specifically adsorbed at the semiconductor surface. The outer Helmholtz plane (*ohp*) marks the distance of closest approach for ions still in the solution. The distance *d* is only a few Ångströms due to the solvation sheet of water molecules surrounding each ion

For $Q_s = 10^{13}$ cm^{-2}, V_H is typically in the order of 0.1~0.5 V.
The Helmholtz capacitance is 10~20 μF cm^{-2}

○ Because of the high conc. of free e^- in **the metal CE**, the space charge region inside the metal is extremely thin (~0.1 nm) and therefore be ignored.
○ The structure of the Helmholtz layer at the metal/electrolyte interface is similar to that for the semiconductor.

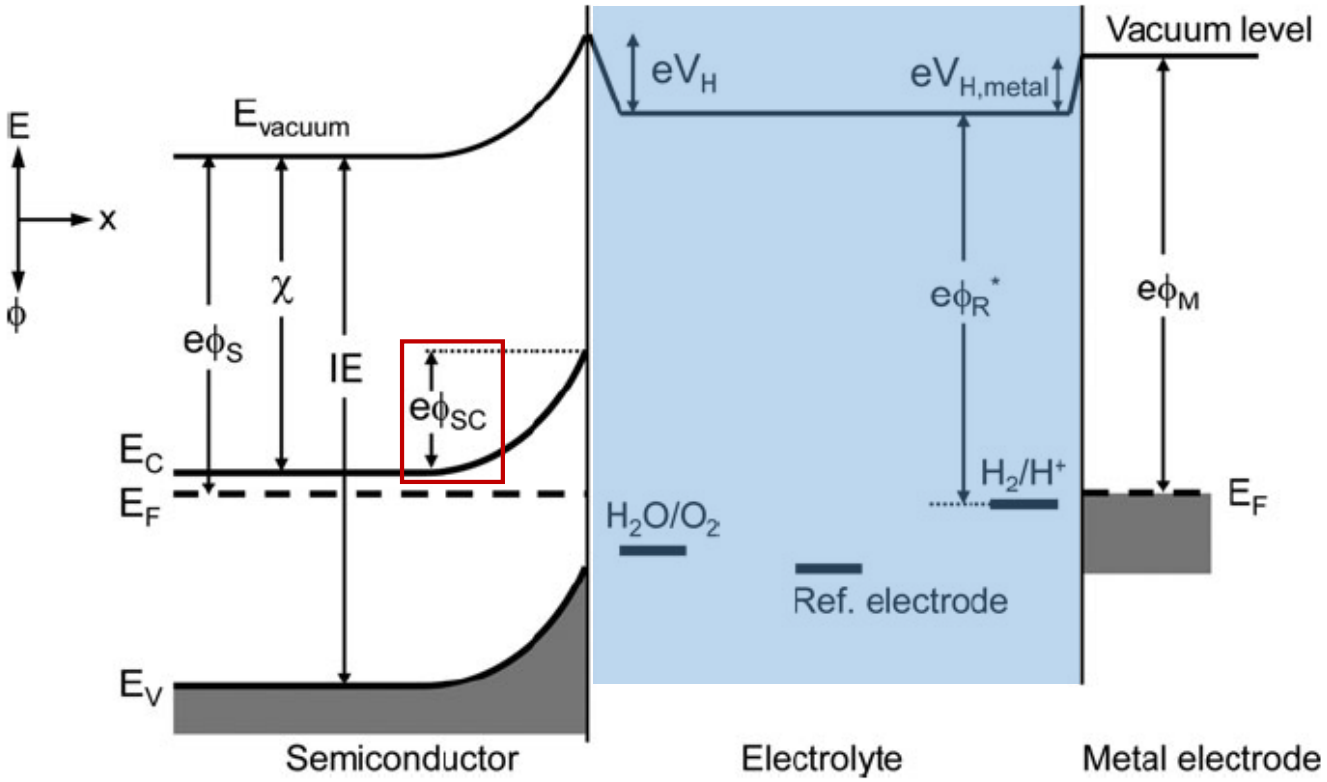

Fig. 2.16 Energy diagram for a PEC cell based on a n-type semiconductor and a metal counter electrode. The vacuum energy level is taken as a reference; this is the energy of an electron in vacuum at infinite distance. The electron affinity (χ) and ionization energy (IE) are materials constants, whereas the semiconductor work function (ϕ_S) also depends on the distance to the surface. Note that a Helmholtz layer is also present at the metal/electrolyte interface

R. Van de Krol and M. Gratzel, *Photoelectrochemical Hydrogen Production*

dark

- The dark current is mainly carried by the majority carriers, (e^-) in the CB for an n-type semiconductor.
- The current flowing is negligible.

light

- The current increases and is dominated by the transfer of minority carriers across the semiconductor /electrolyte interface.

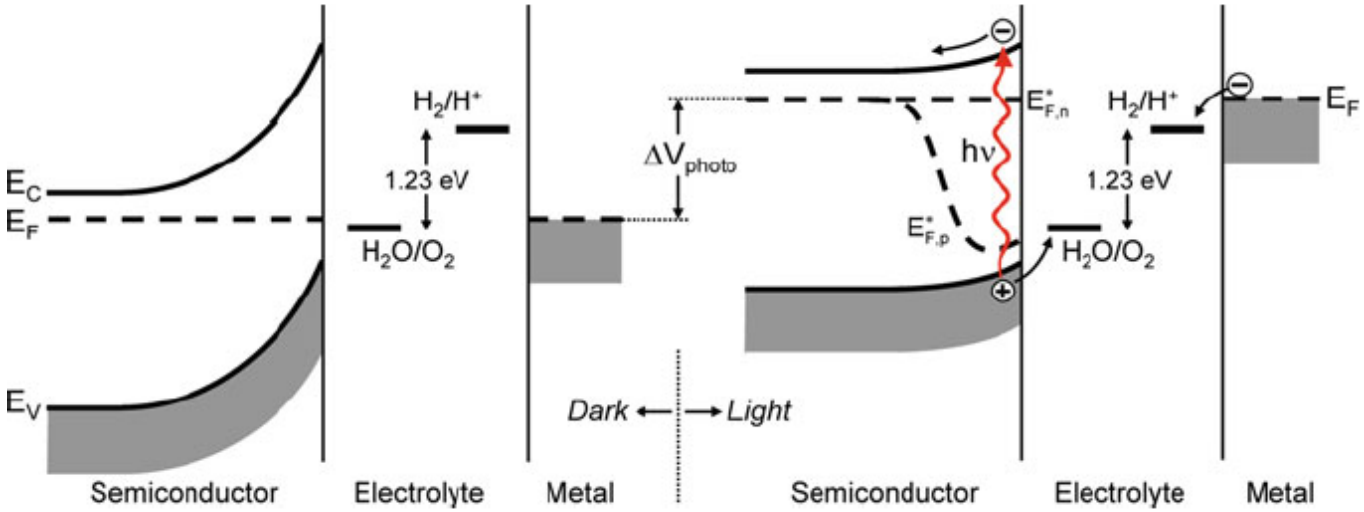

Fig. 2.20 Band diagram for a PEC cell based on an n-type semiconducting photoanode that is electrically connected to a metal counter electrode; in equilibrium in the dark (*left*) and under illumination (*right*). Illumination raises the Fermi level and decreases the band bending. Near the semiconductor/electrolyte interface, the Fermi level splits into quasi-Fermi levels for the electrons and holes

Under illumination, e^-/h^+ pairs are created and the E_F increases w/ ΔV_{photo} (internal photovoltage). The system is no longer in equilibrium: The use of a single E_F is no longer appropriate. Instead, **quasi-Fermi levels** is formed for charge carriers.

R. Van de Krol and M. Gratzel, *Photoelectrochemical Hydrogen Production*

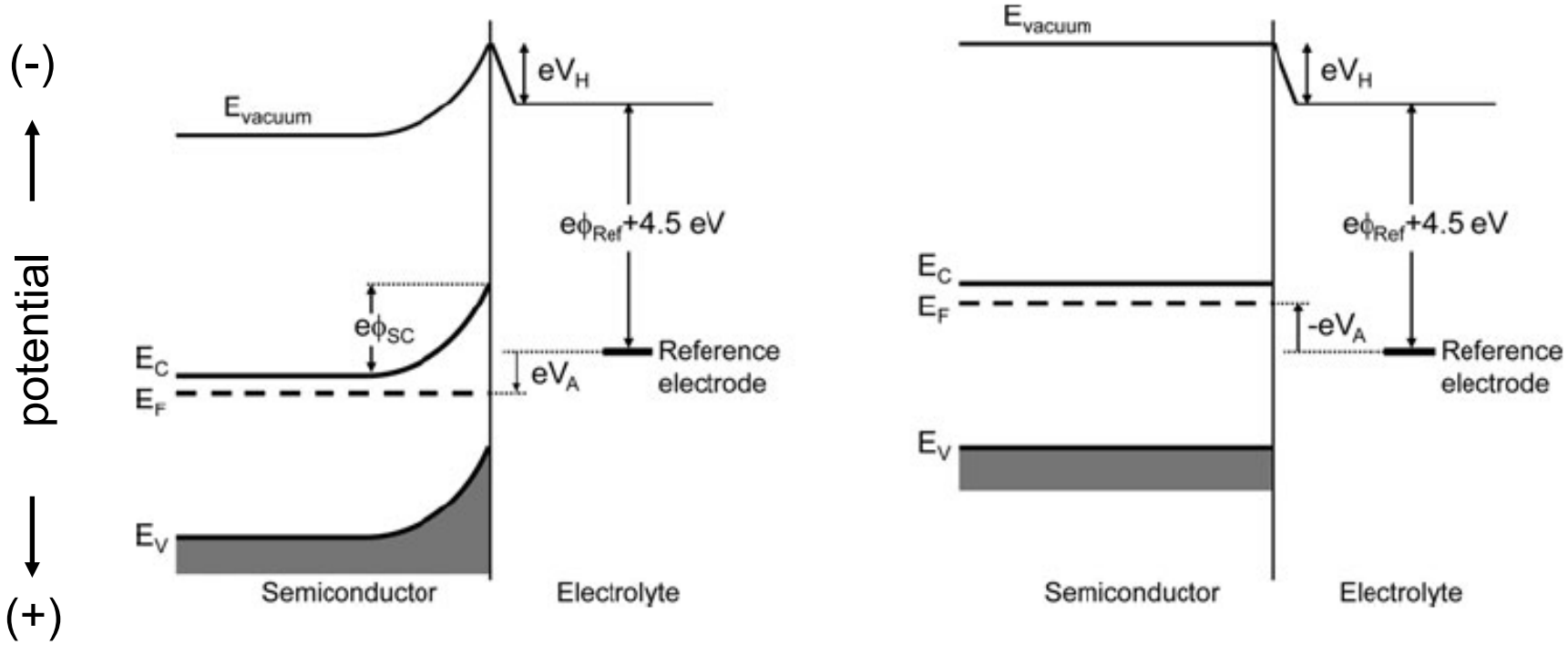

Fig. 2.17 Effect of applying a bias voltage (V_A) to an n-type semiconductor electrode. Any change in applied potential falls across the space charge layer, whereas V_H remains constant. In the picture on the left, a positive potential is applied to the semiconductor. When a sufficiently negative bias is applied, the band bending can be reduced to zero (*right*)

R. Van de Krol and M. Gratzel, *Photoelectrochemical Hydrogen Production*

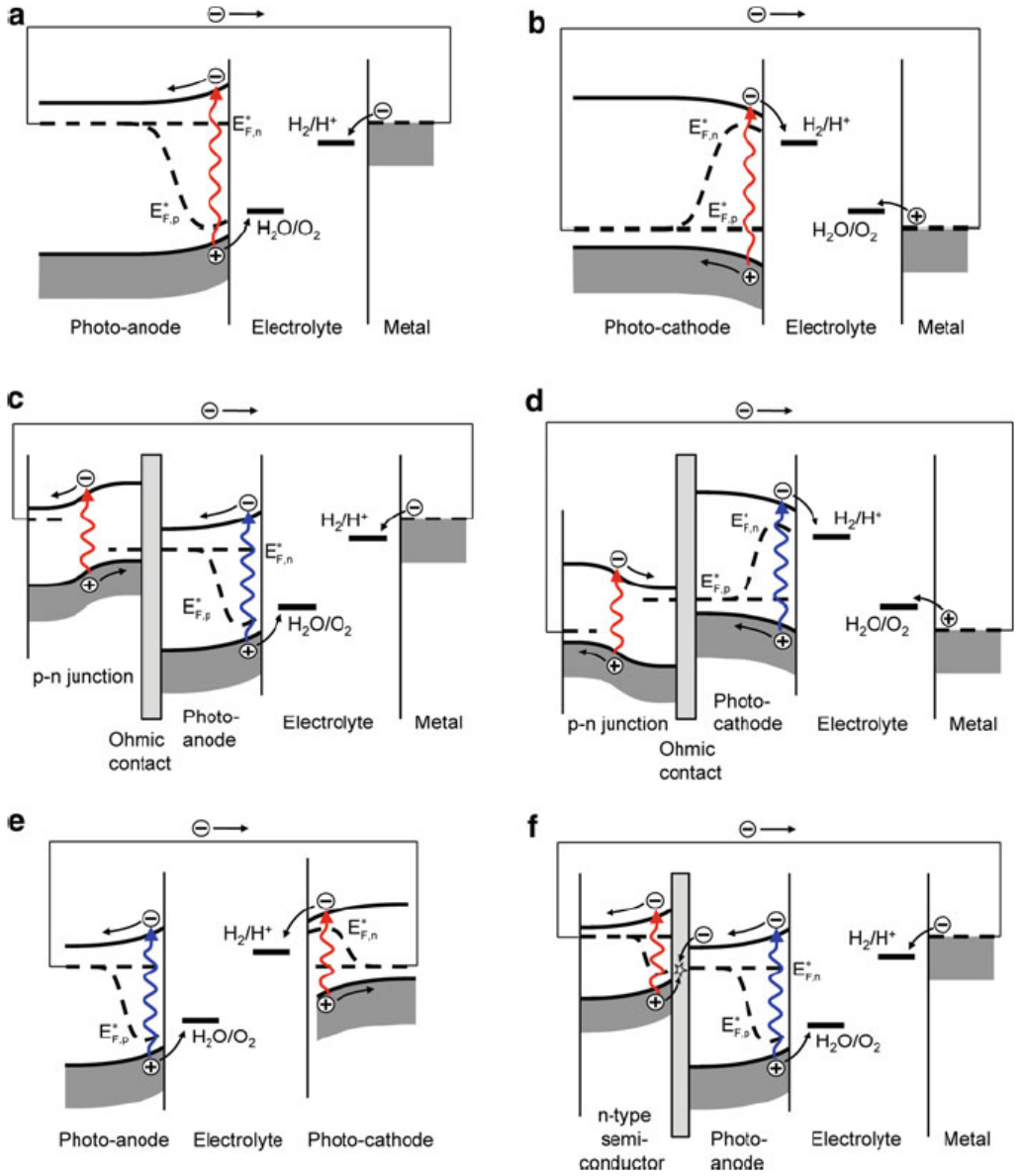

Fig. 2.25 Examples of possible PEC configurations under illumination. *Top row*: Standard single-semiconductor devices based on a photoanode (**a**) or photocathode (**b**) with a metal counter electrode. *Middle row*: Monolithic devices based on a photoanode (**c**) or photocathode (**d**) biased with an integrated p–n junction. *Bottom row*: p–n junction photoelectrochemical device (**e**), and an n–n heterojunction PEC device based on a photoanode deposited on top of a second n-type semiconductor that "boosts" the energy of the electrons (**f**)

R. Van de Krol and M. Gratzel, *Photoelectrochemical Hydrogen Production*

5. Hematite (Fe_2O_3)

- 16.8% converting solar energy into H_2
- Highly stable in alkaline solution
- Absorption of visible light
- Cheap and environmentally benign

- A flat band potential (V_{fb}) too low in energy for H_2 evolution
- A large requisite η for O_2 evolution
- A relatively low absorption coefficient, requiring 400~500 nm thick film for complete light absorption
- Poor majority carrier conductivity
- A short diffusion length (L_D = 2~4 nm) of minority carriers (ultrafast recombination), requiring high doping level to increase the ionized donor conc. and conductivity. This in turn reduces the width of the space-charge layer.

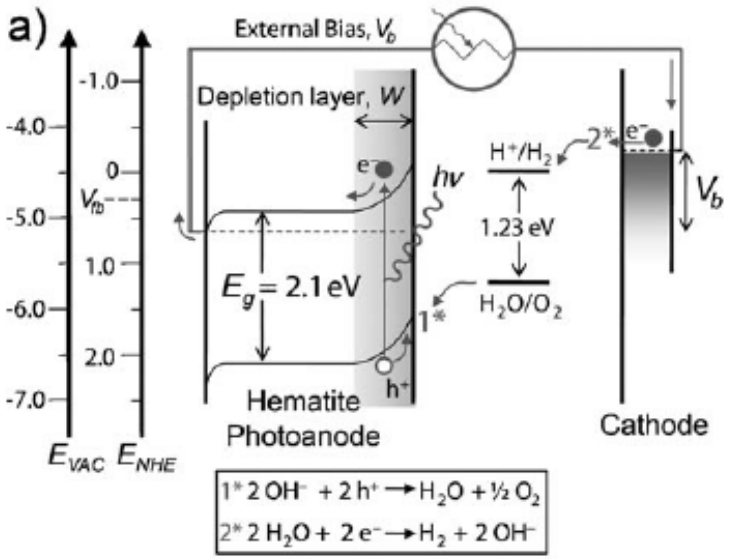

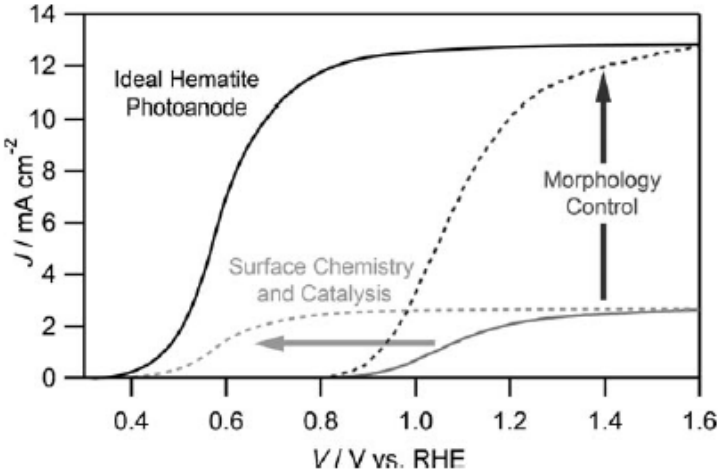

Figure 3. The two-part strategy for improving hematite performance is shown with respect to the photocurrent density, *J*, vs. voltage behavior for an idealized hematite photoanode (solid black trace) compared to the typical performance (solid grey trace) under AM 1.5G 100 mW cm^{-2} simulated sunlight, and the expected effects of improving the surface chemistry and the morphology.

ChemSusChem, **2011**, *4*, 432-449

• Solar-to-hydrogen efficiency (η_{STH})

(1) $$\eta_{STH} = \frac{P^{out}_{electrical} - P^{in}_{electrical}}{P_{light}} = \frac{j_{photo}(1.23 - V_{bias})}{P_{light}}$$

AM 1.5G incident sunlight (P_{light} = 1000 W/m^2)

For 10% efficiency target for economically viable PEC cells,,
a photocurrent (j_{photo}) of ~8 mA/cm^2 is required.

$\eta_{STH} = 1.23 \times j_{photo}$ at no applied bias

(2) $$\eta_{STH} = \frac{\Phi_{H2} G^{o}_{g,H2}}{P_{light}}$$

Φ_{H2} : the rate of H_2 evolution at the illuminated area (mol/s/m^2)

$G^{o}_{g,H2}$: the Gibbs free energy of formation of H_2 (237 kJ/mol)

• Incident photon-to-current conversion efficiency (IPCE)

Quantum efficiency as a function of wavelength

$$IPCE(\lambda) = \frac{hc}{e}\left(\frac{j_{photo}(\lambda)}{\lambda P(\lambda)}\right)$$

• Total solar photocurrent

$$J_{solar} = \int (IPCE(\lambda) \times \Phi(\lambda) \times e)\, d\lambda$$

$\Phi(\lambda)$: The photon flux of sunlight (photon/m^2/s)

Nanostructural engineering

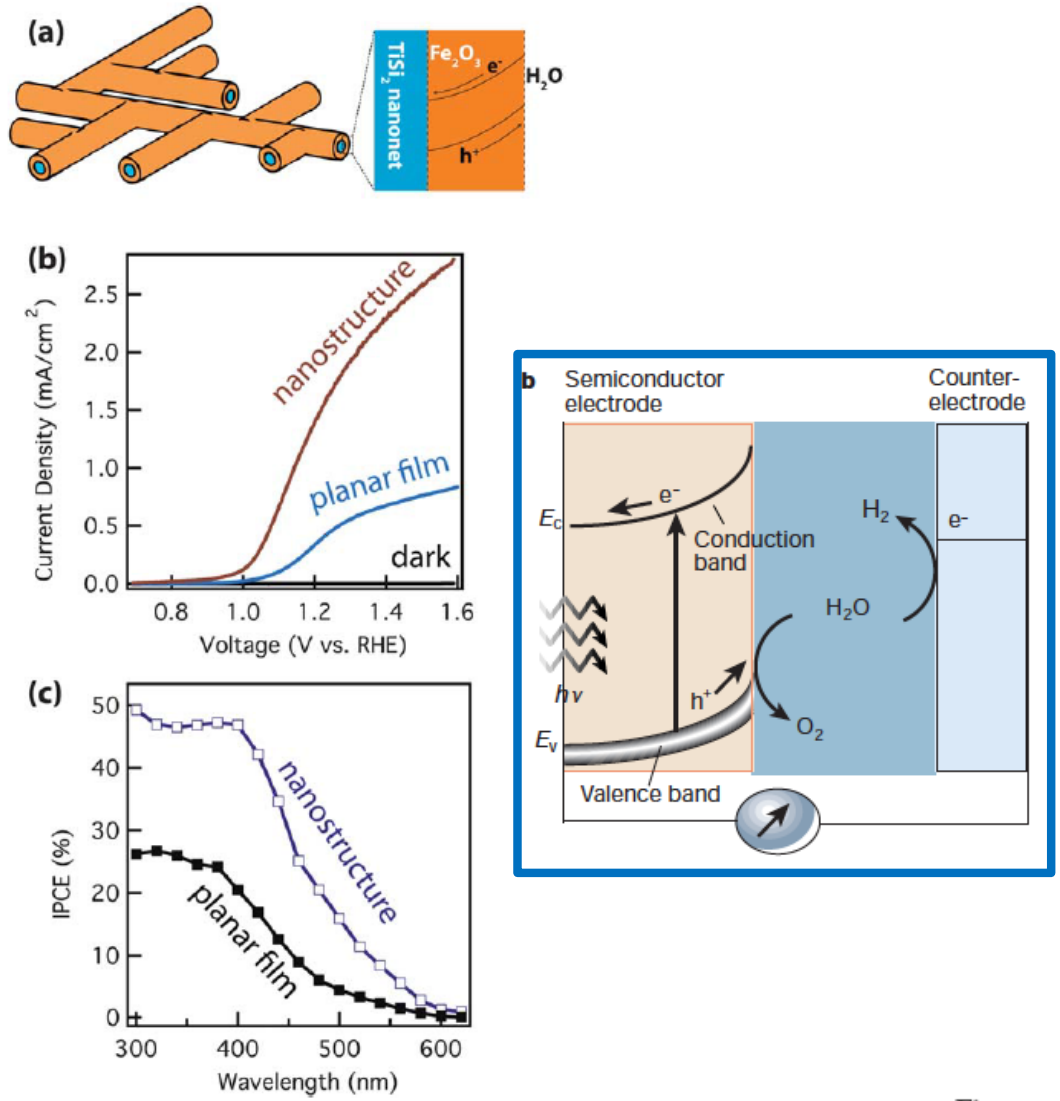

Fig. 3 Nanonet–hematite nanostructures and their performance for water splitting. (a) A schematic representation of the design. (b) The comparison of the photoelectrochemical performance between the nanostructure and planar hematite. (c) The external quantum efficiency comparison (measured at 1.53 V *vs.* RHE). Worth noting is that the hematite is without any intentional doping. Adapted from Lin *et al.*, *J. Am. Chem. Soc.*, 2011 (ref. 41).

Energy Environ. Sci., **2011**, *4*, 4862-4869

Doping

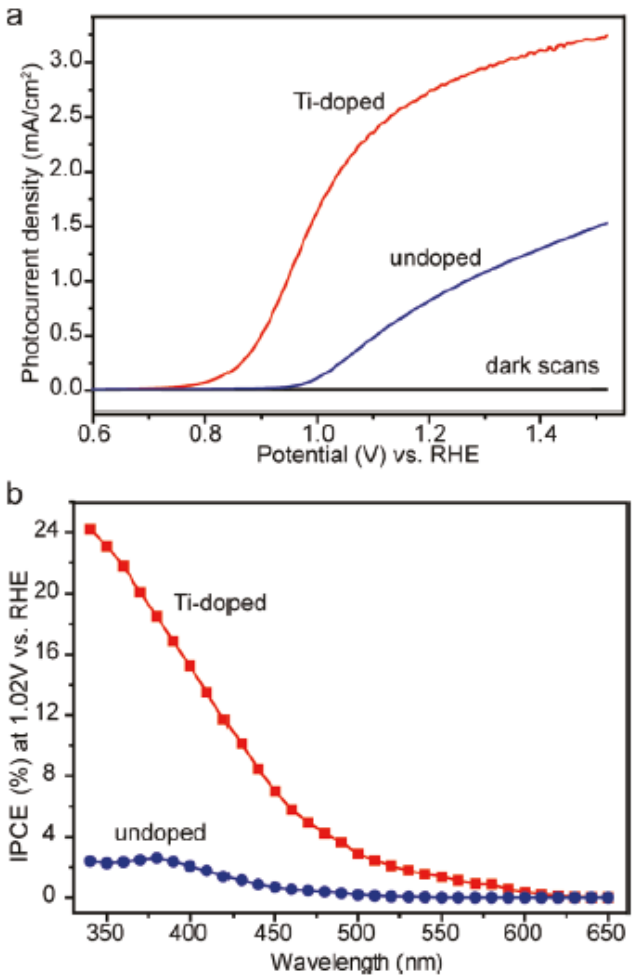

Figure 4. (a) Comparison of photocurrent densities collected for optimized undoped and Ti-doped α-Fe_2O_3 films. (b) IPCE spectra of these two films collected at 1.02 V vs RHE.

IPCE: Incident photon-to-current conversion efficiencies

Nano Lett., **2011**, *11*, 3503-3509

PEC + OER catalyst: OER is still very sluggish in the absence of catalyst

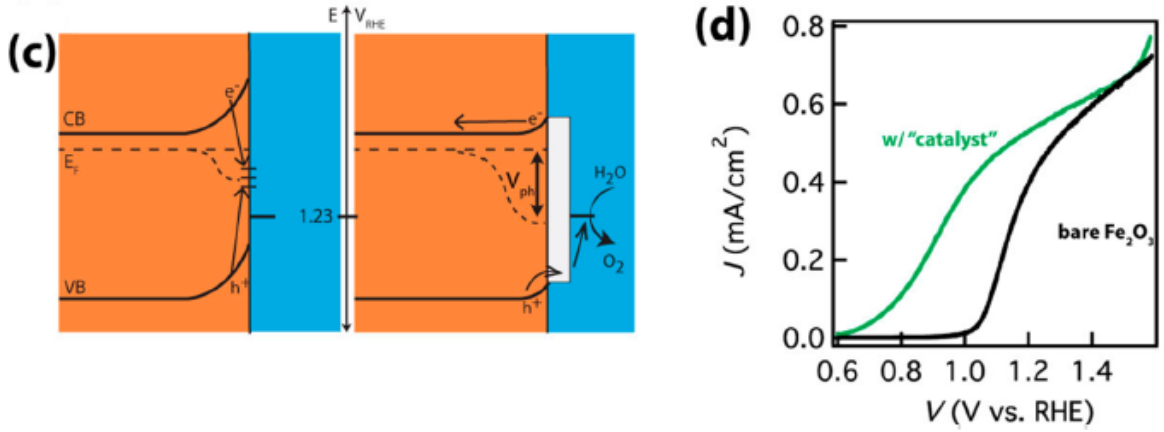

separate chambers (b). The charge separation mechanism in photoelectrochemical systems relies on the built-in field to drive photoexcited electrons and holes toward opposite directions (c). The performance of a representative photoanode system by hematite (α-Fe_2O_3) with and without water oxidation catalyst (amorphous $NiFeO_x$) is shown in (d). Adopted from ref 29 with permissions.

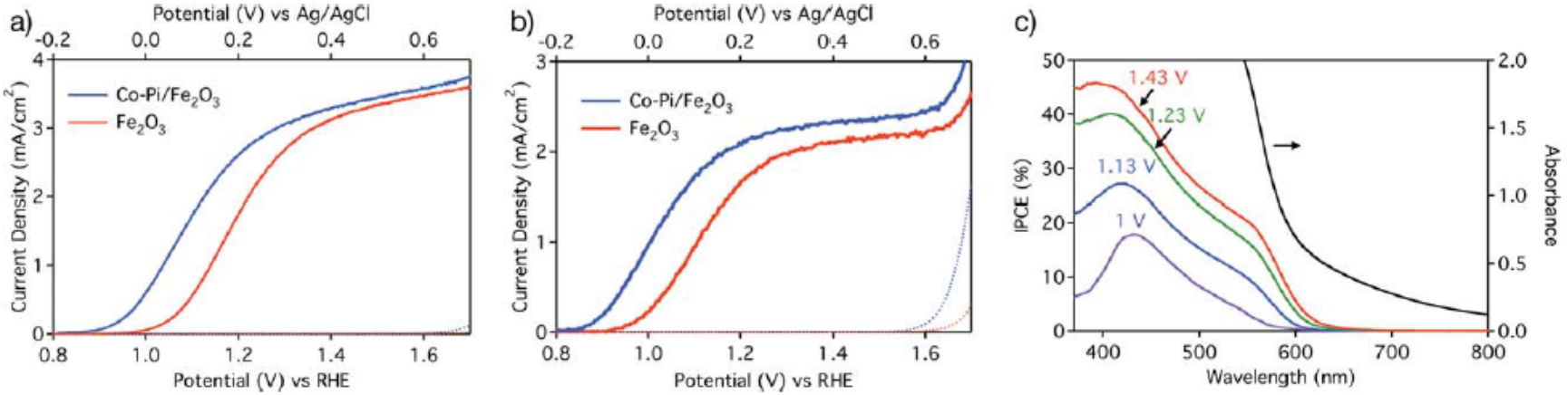

Fig. 4 (a and b) Dark-current (dotted) and photocurrent (solid) densities of Co–Pi/α-Fe_2O_3 photoanodes prepared by photo-assisted electrodeposition (blue) and of the parent α-Fe_2O_3 photoanodes (red) illustrating the effect of Co–Pi on two α-Fe_2O_3 photoanodes with qualitatively different responses. (c) Incident photon-to-current conversion efficiencies (IPCEs, colored) and absorption spectrum (black) of a Co–Pi/α-Fe_2O_3 photoanode prepared by photo-assisted electrodeposition.

J. Phys. Chem. Lett. **2015**, *6*, 4083-4088., *Energy Environ. Sci.*, **2011**, *4*, 1759-1764

6. Electrolysis: application for redox flow battery

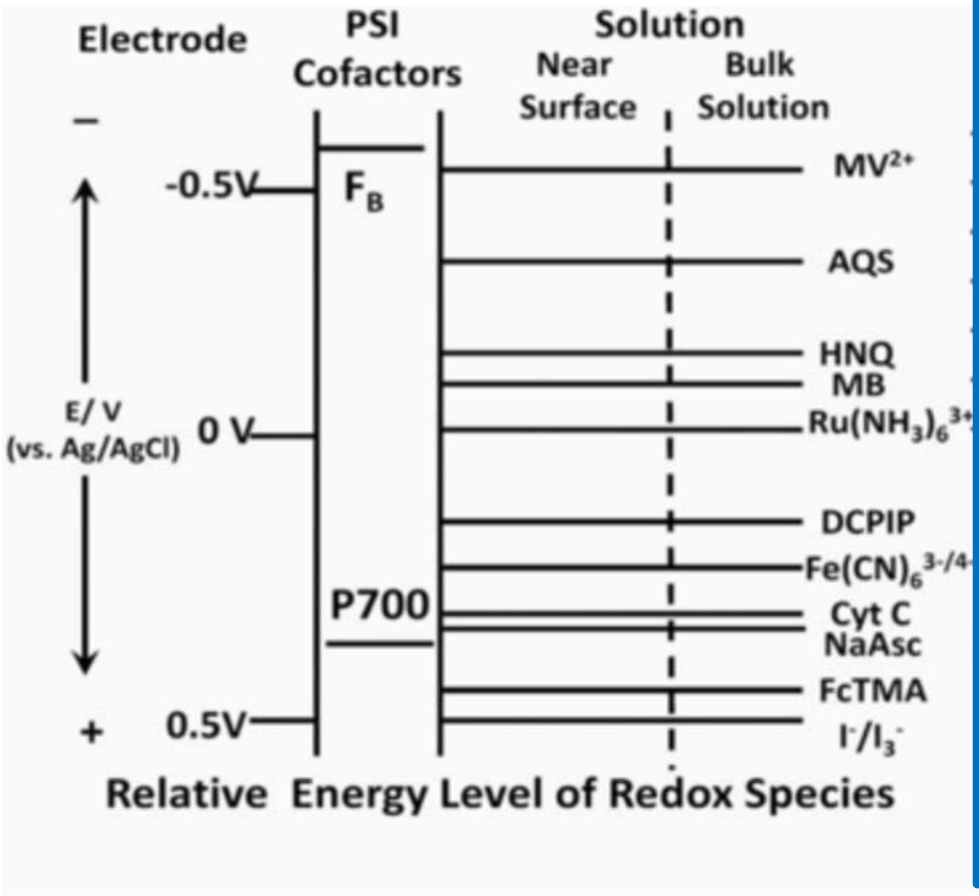

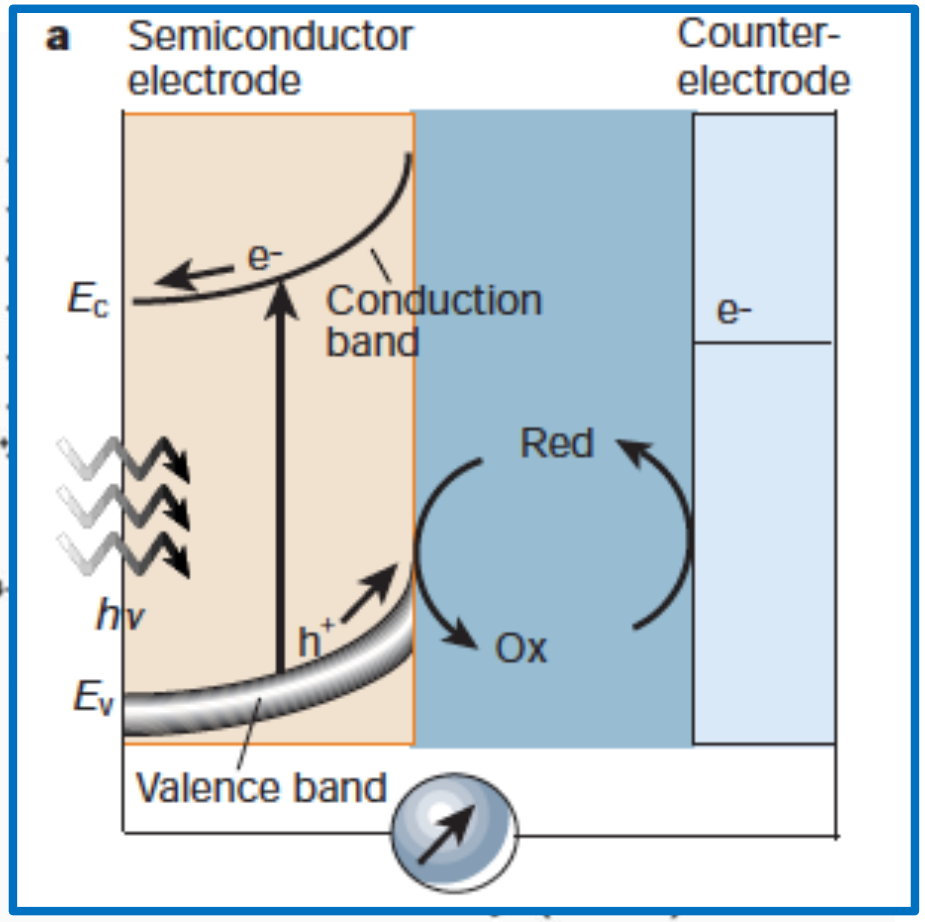

M. Gratzel, *Nature* **2011**, *414*, 338-344.
J. Electrochem. Soc., **2013**, *160*, H315-H320

Interfacial electron transfer

- The e^- transfer is much faster than ionic reorganization (solvation, probability distribution of density of state for redox species).
- The probability of e^- transfer decreases if E_{red} is too far above E_V^S (which is markedly different from the behavior of metal electrodes showing a continuous increase in current w/ applied potential)

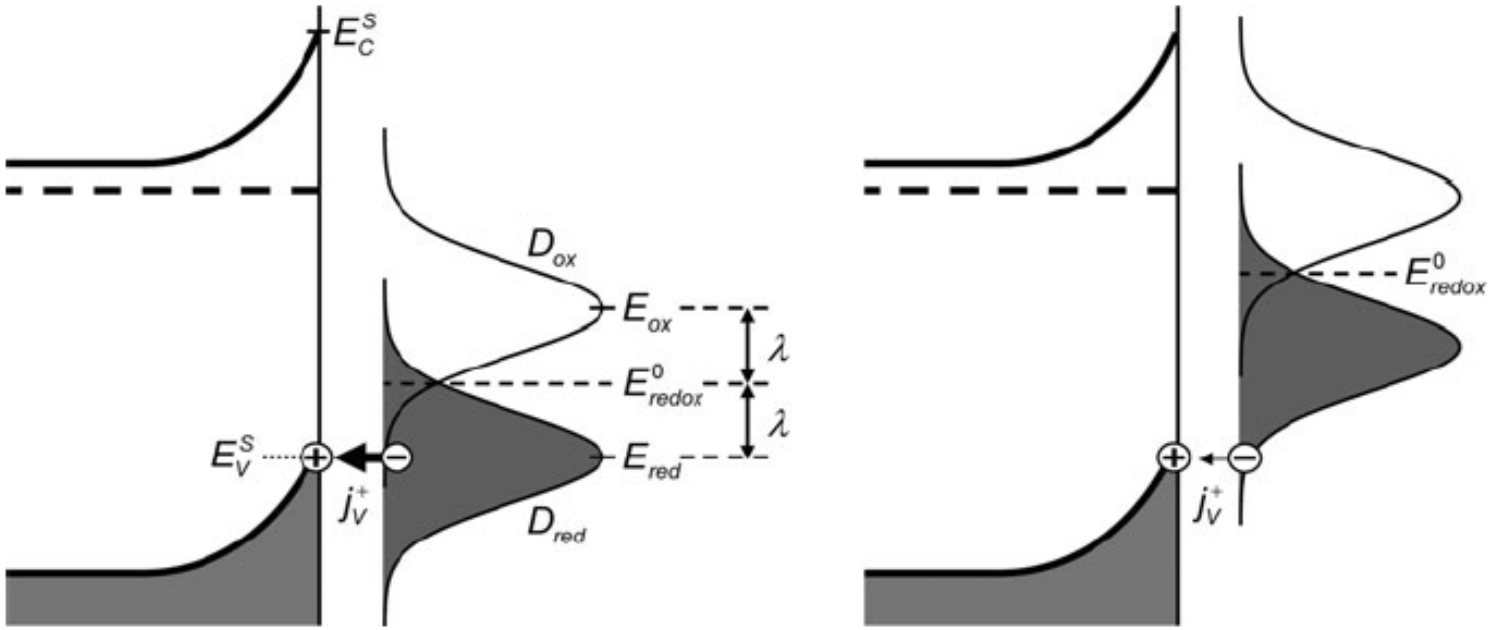

Fig. 2.19 Energy level model for electron transfer from a redox species in the electrolyte to a photogenerated hole in the semiconductor valence band. The density of states D_{red} depend on the concentration of the reductant species according to $D_{red} = c_{red} W_{red}(E)$. A large overlap of the redox DOS with the energy of the hole (*left*) gives higher currents than a small overlap (*right*)

R. Van de Krol and M. Gratzel, *Photoelectrochemical Hydrogen Production*

Redox flow batteries for ESS*

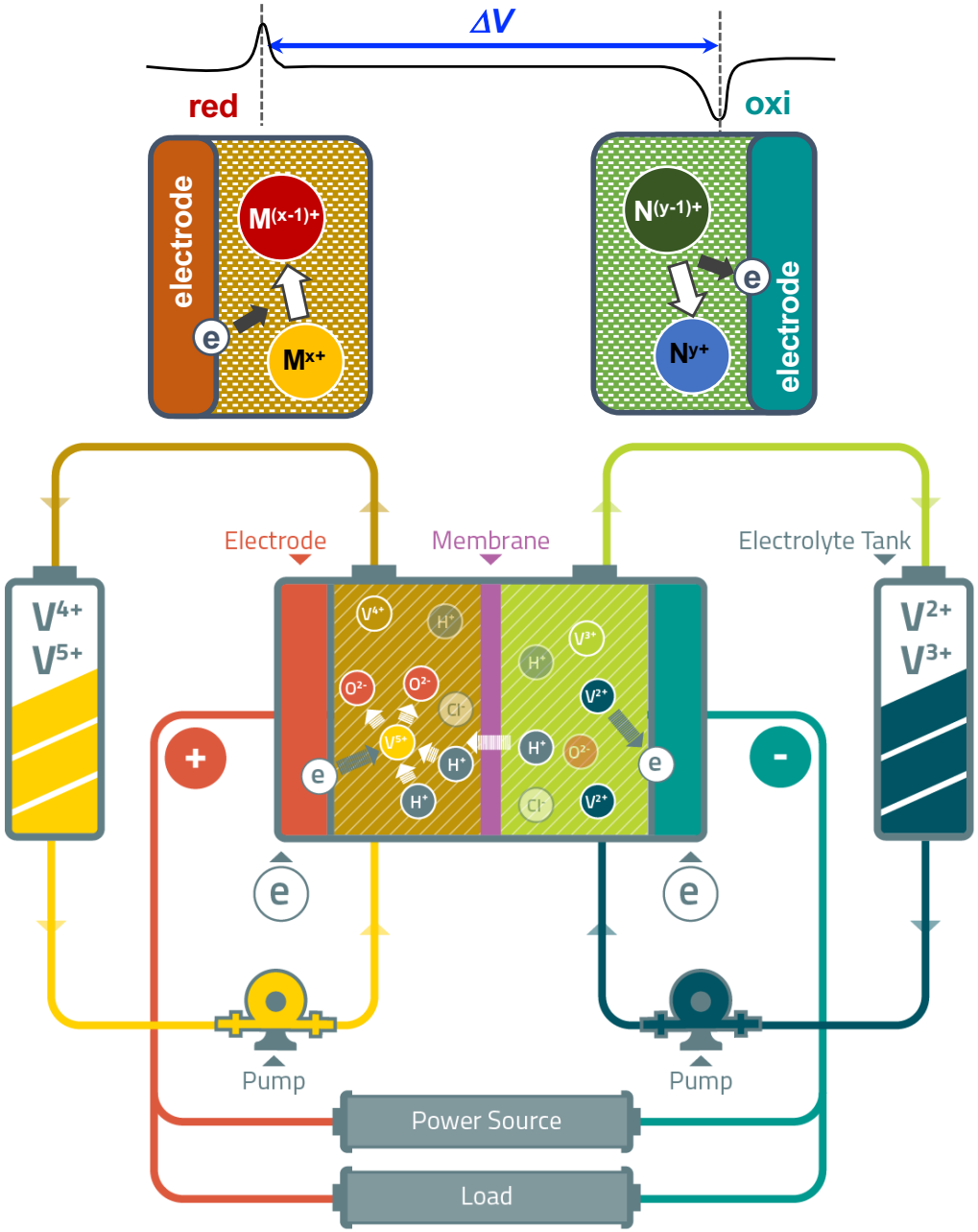

*ESS: Energy Storage System

Solubility of reversible redox couples in aqueous media

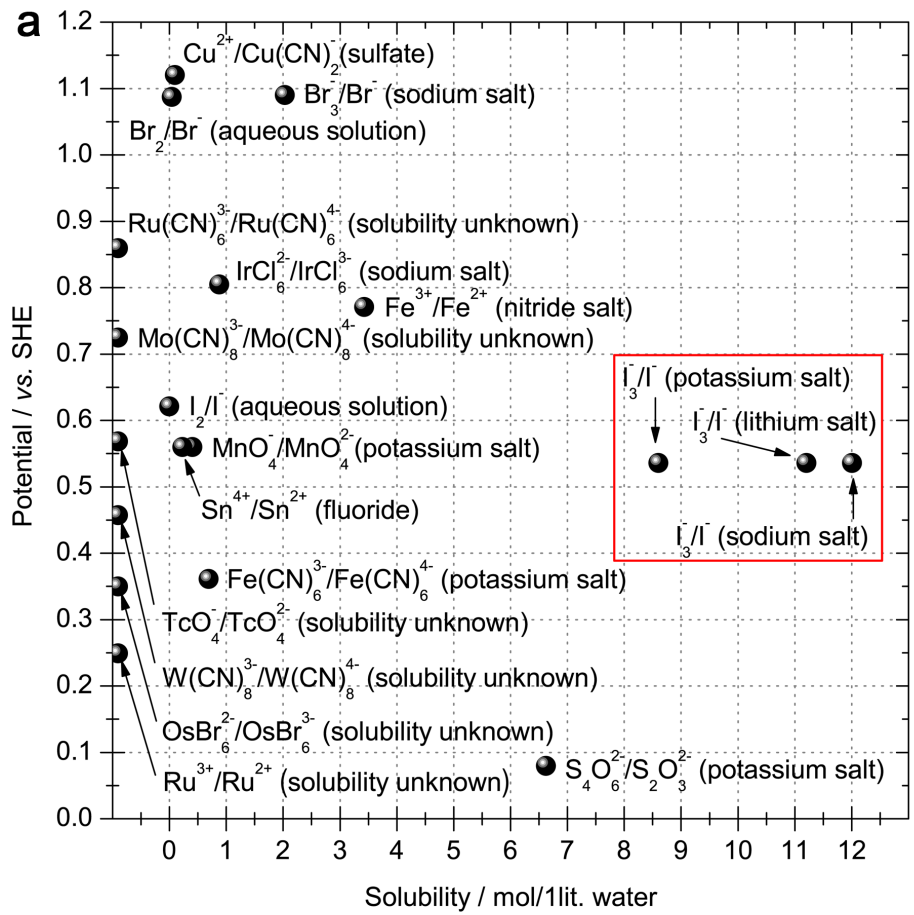

1. Solubility oc <u>Energy density</u>

I_3^-/I^- redox couple: ~8.5 mol L^{-1} with K^+ salt

2. <u>Redox potential</u>: avoid water electrolysis

I_3^-/I^- redox couple: ~0.536 V vs. SHE

3. pH: close to 7 (neutral solution)

I_3^-/I^- aqueous cathode: pH = 6–7

Working concept of I_3^-/I^- redox reaction in the aqueous Li-I_2 battery

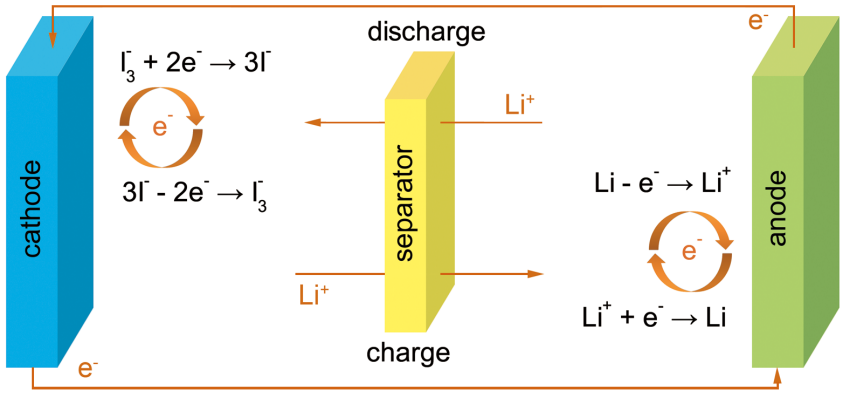

Cell reaction

Aqueous cathode: $I_3^- + 2e^- \leftrightarrow 3I^-$

Li anode: $\leftrightarrow$ $2Li$ $2Li^+ + 2e^-$

Total cell reaction: $2Li + I_3^- \leftrightarrow 2Li^+ + 3I^-$

(E = 3.5 V vs. Li^+/Li)

Preparation of I_3^-/I^- aqueous cathode

I_2 (s) + I^- $\leftrightarrow$ I_3^-, K = 723

0.1 M I_2 and 1 M of KI in aqueous solution (≈ 0.1 M of I_3^-)

Electrochemical performance of aqueous Li-I_2 batteries

Aqueous cathode: 0.08 M of I_2 in 1 M KI and 0.03 M LiI

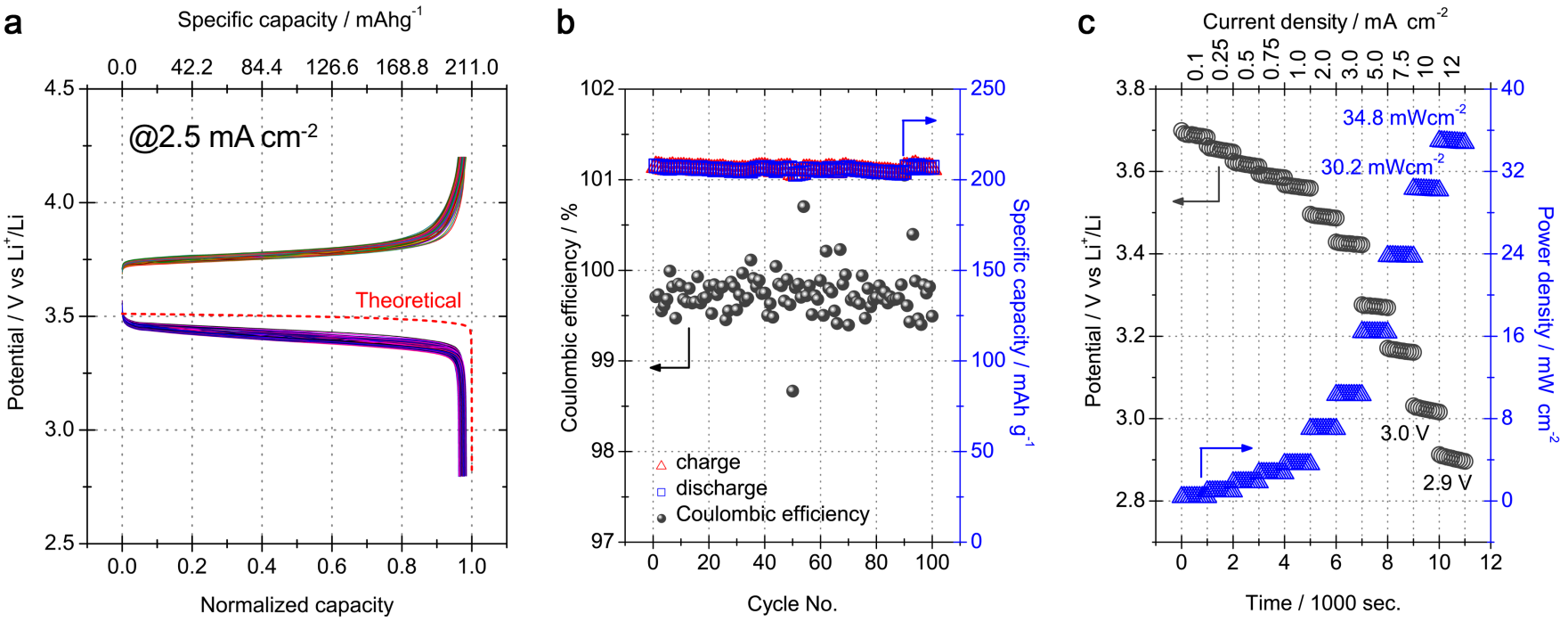

Specific capacity: 207 mAh g^{-1}
i.e. 98% of the theoretical capacity

99.6% capacity retention
> 99.5% Coulombic efficiency

Power density
34.8 mW cm^{-2} at 12 mA cm^{-2}
(discharge potential: 2.9 V)

The aqueous Li-I_2 battery is noticeably different from either the *conventional all-solid-state or non-aqueous electrolyte -based Li-I_2 batteries*, which have performed at *extremely low discharge current rate* or shown *low Coulombic efficiency with the formation of a LiI layer*.

Zhao, Y.; Wang, L.; Byon, H. R., *Nature Communications* **2013**, *4*, 1896.

Aqueous Li-I flow cell

Total 0.5 mL of 0.5 M of LiI aqueous cathode

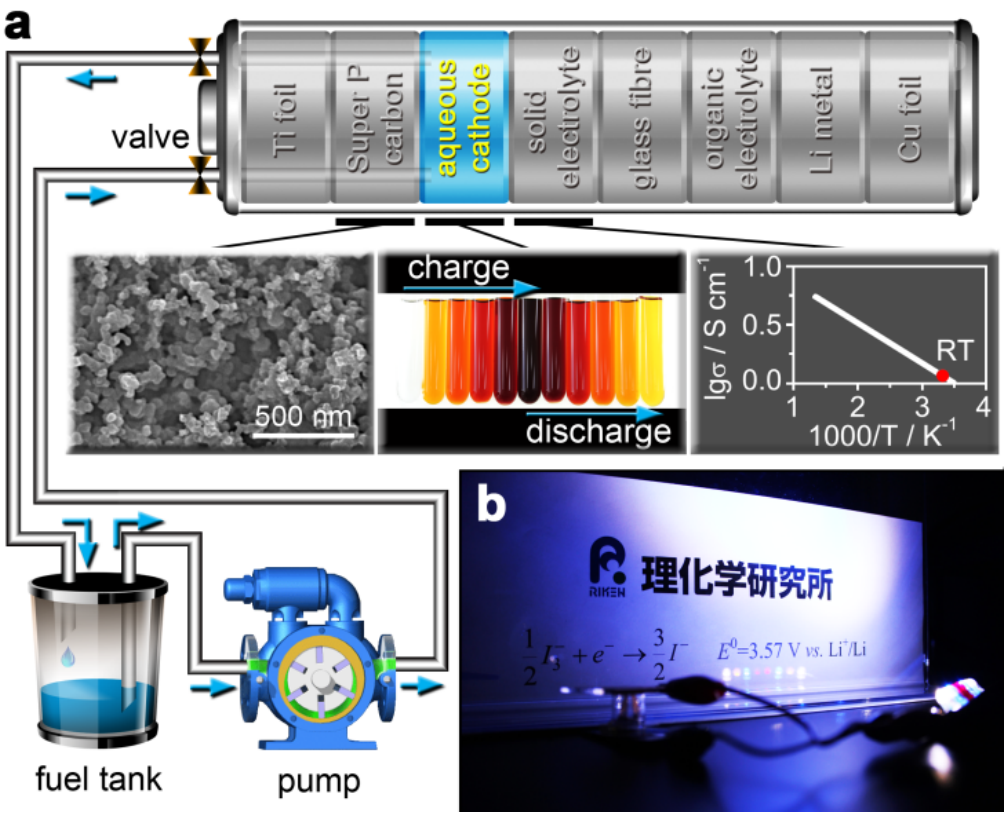

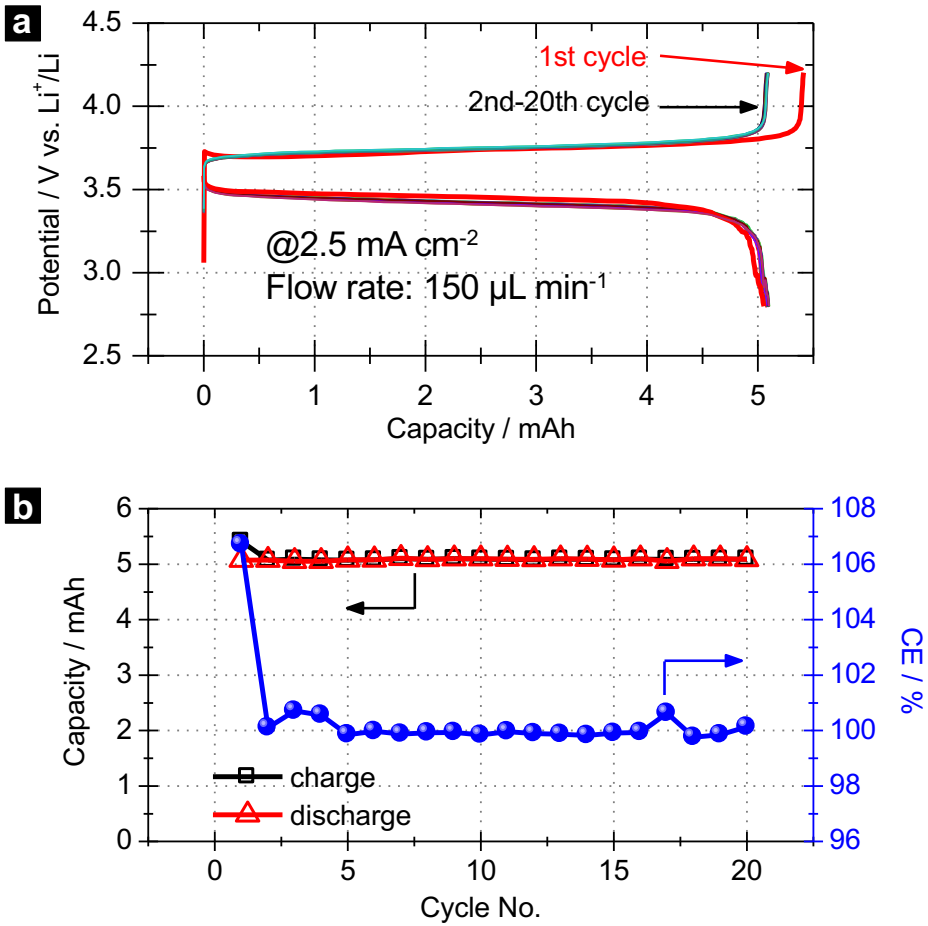

Zhao, Y.; Byon, H. R., *Adv. Energy Mater.* **2013**, 3, 1630-1635.

Solar-stimulated redox battery

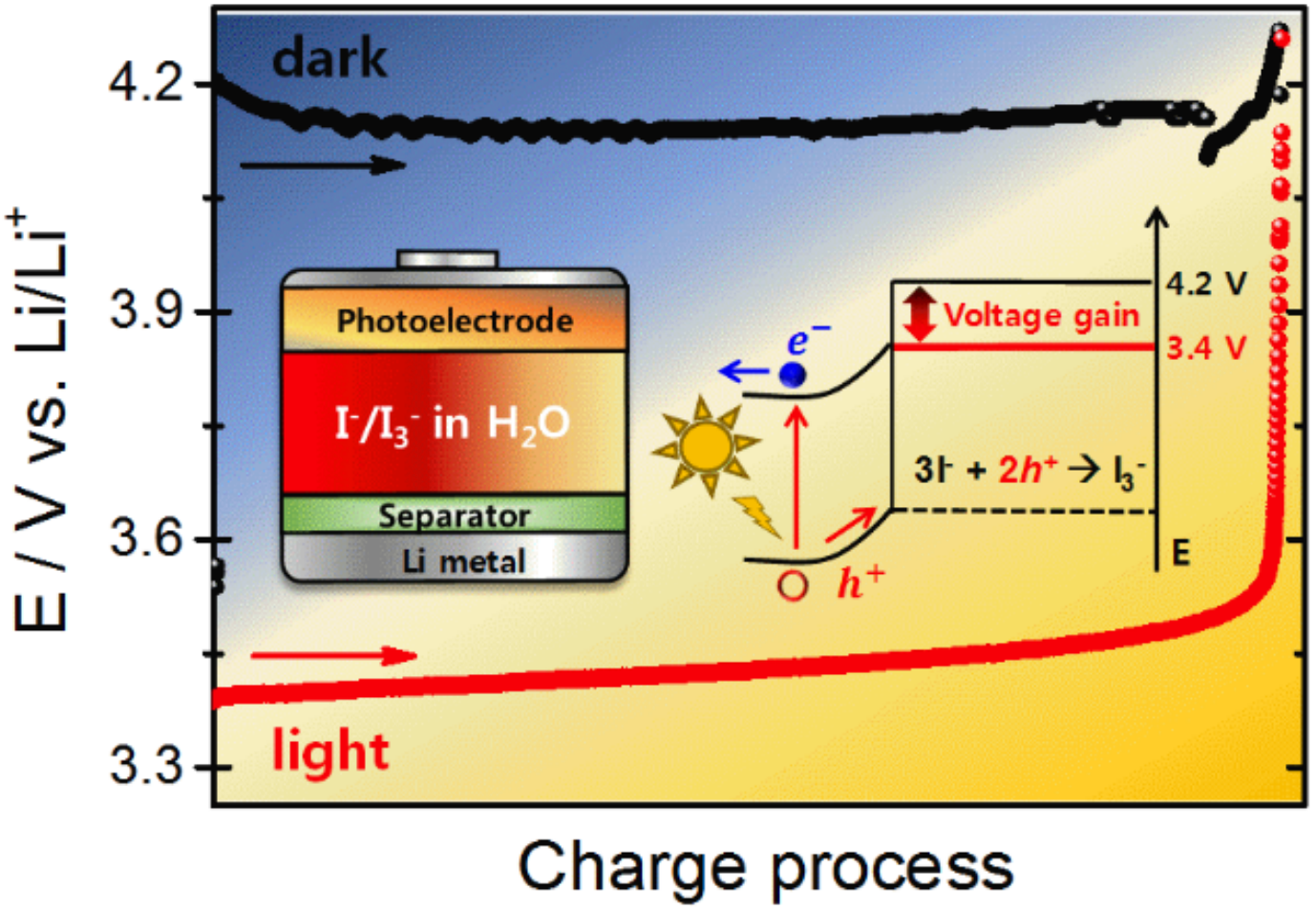

Electrochemical oxidation

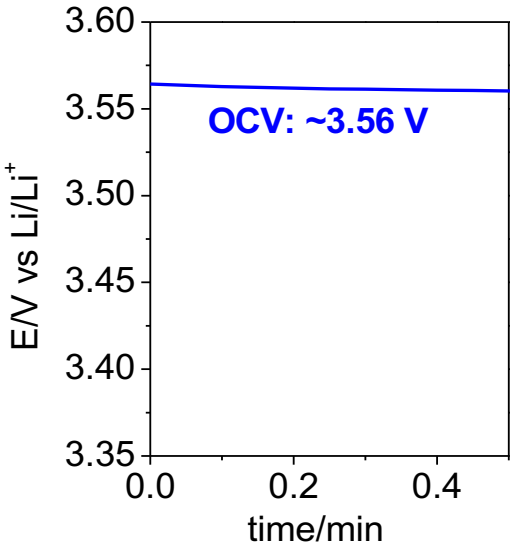

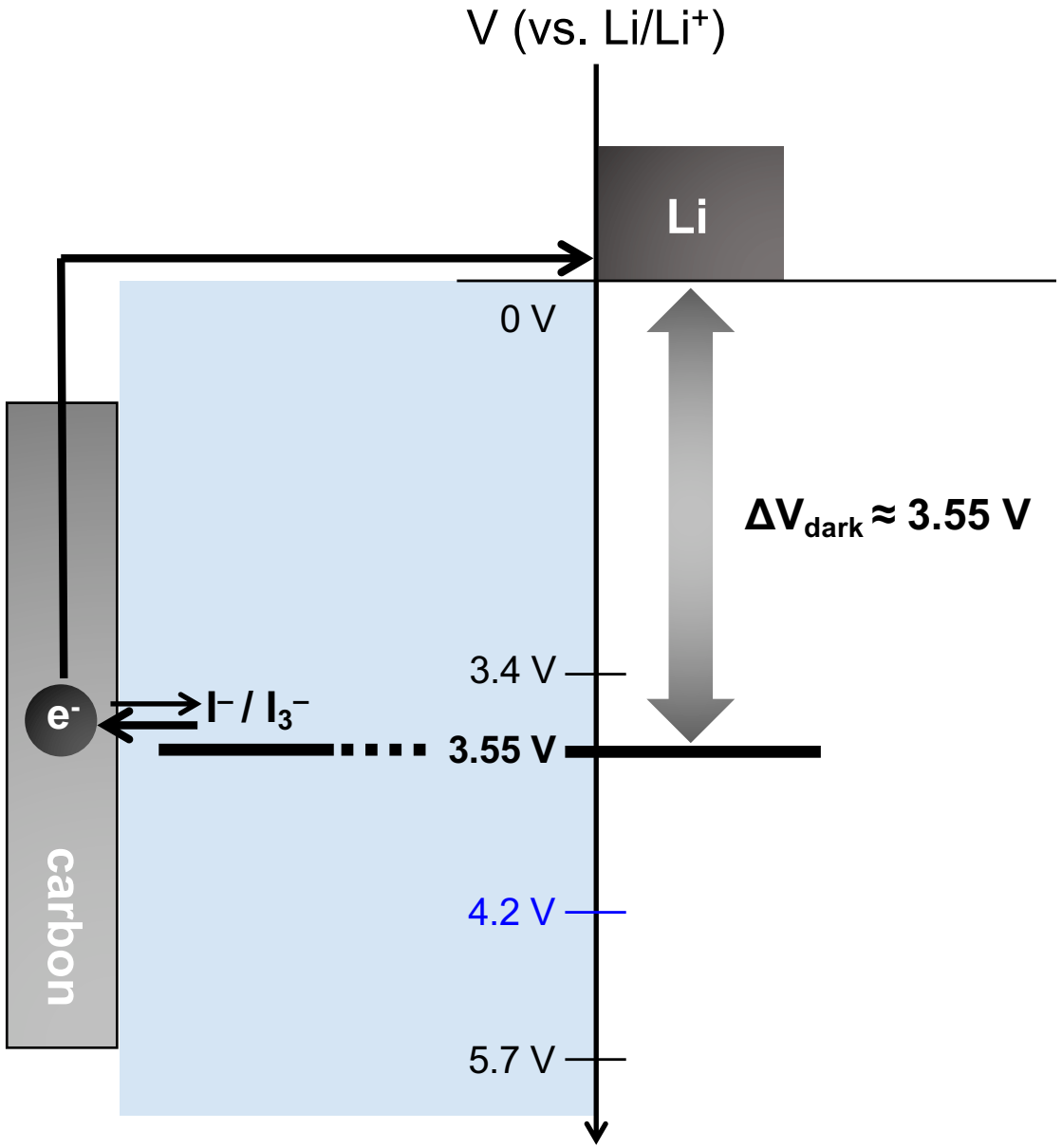

Photoelectrochemical reaction for oxidation

α-Fe_2O_3 + hν → α-Fe_2O_3 + e^- + h^+

$3I^- + 2h^+ \rightarrow I_3^-$

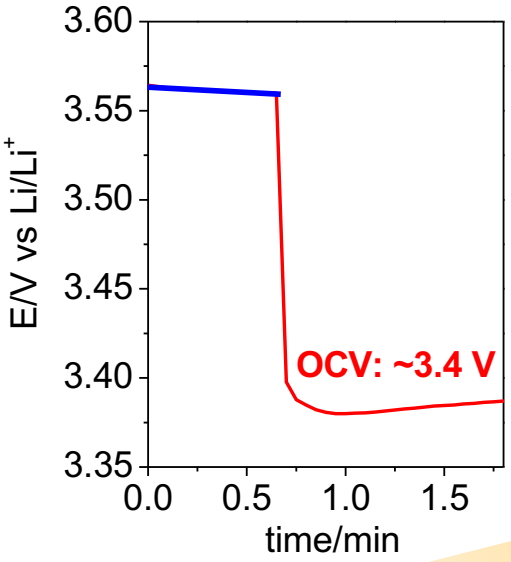

Li-I_2 battery w/ hematite electrodes at open circuit voltages

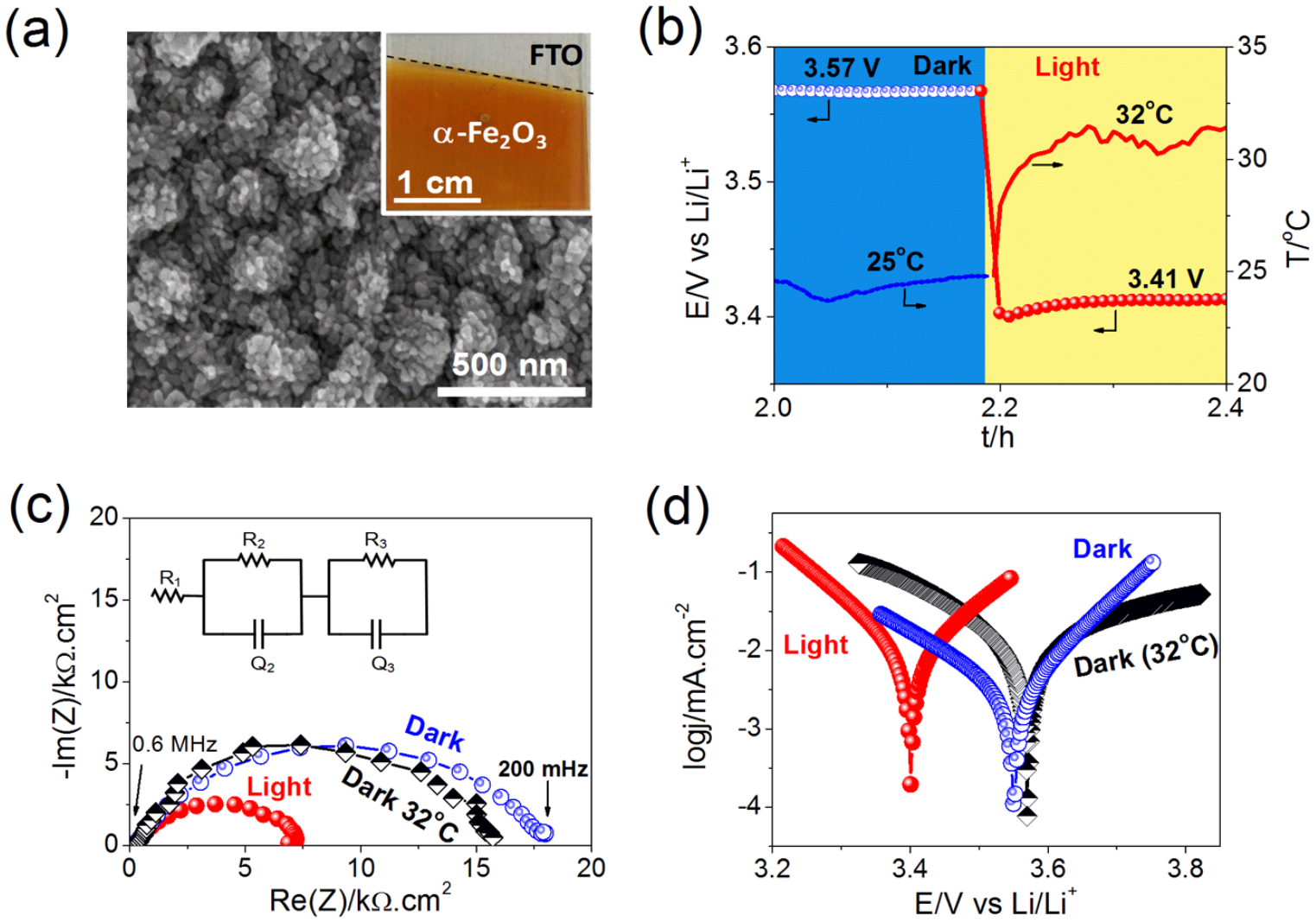

Nikiforidis, G.; Tajima, K.; Byon, H. R., *ACS Energy Lett.* **2016**, *1*, 806-813.

Charge efficiency for photo-assisted Li–I_2 battery

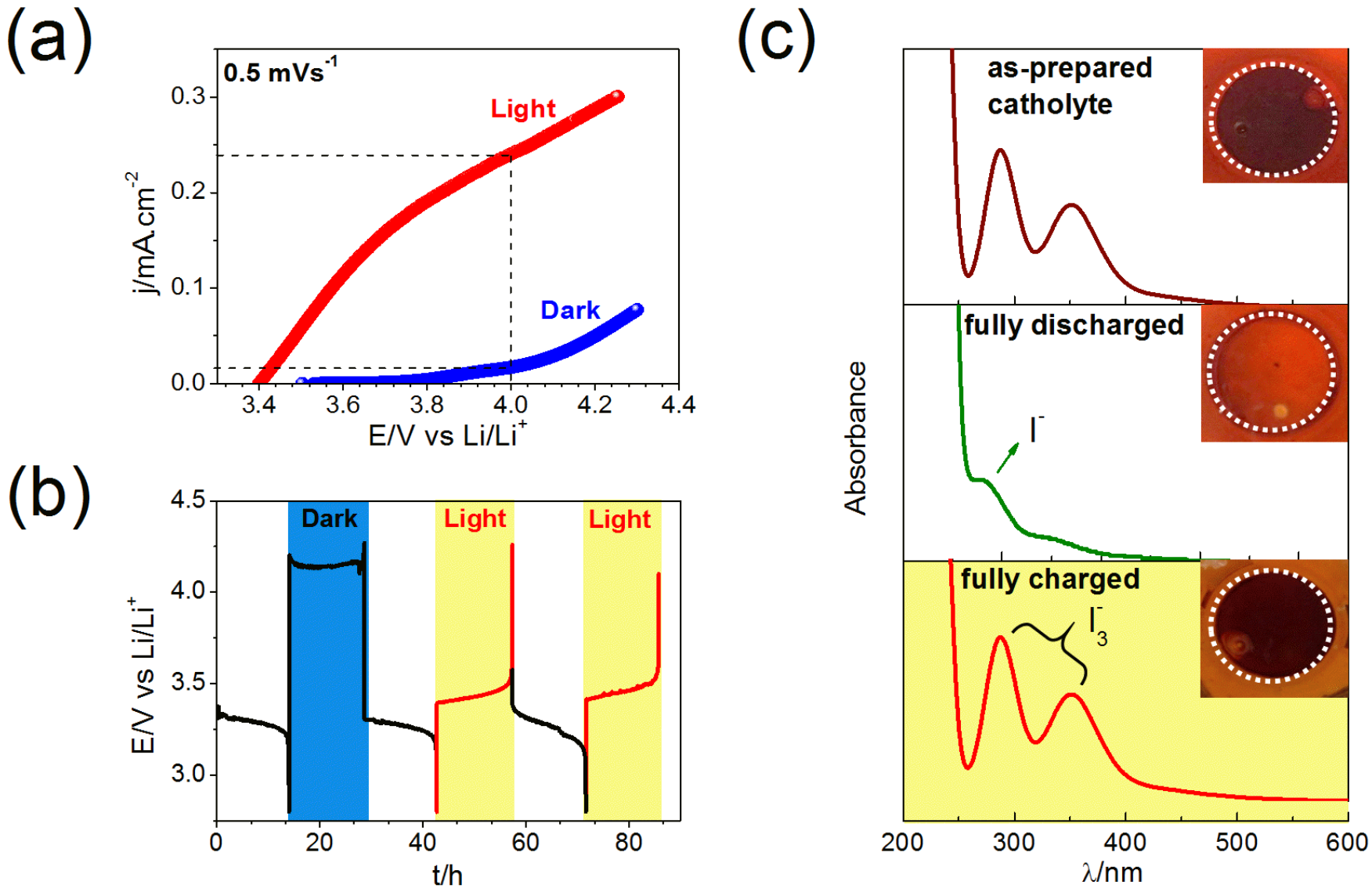

Energy efficiency with photo-assisted electrode

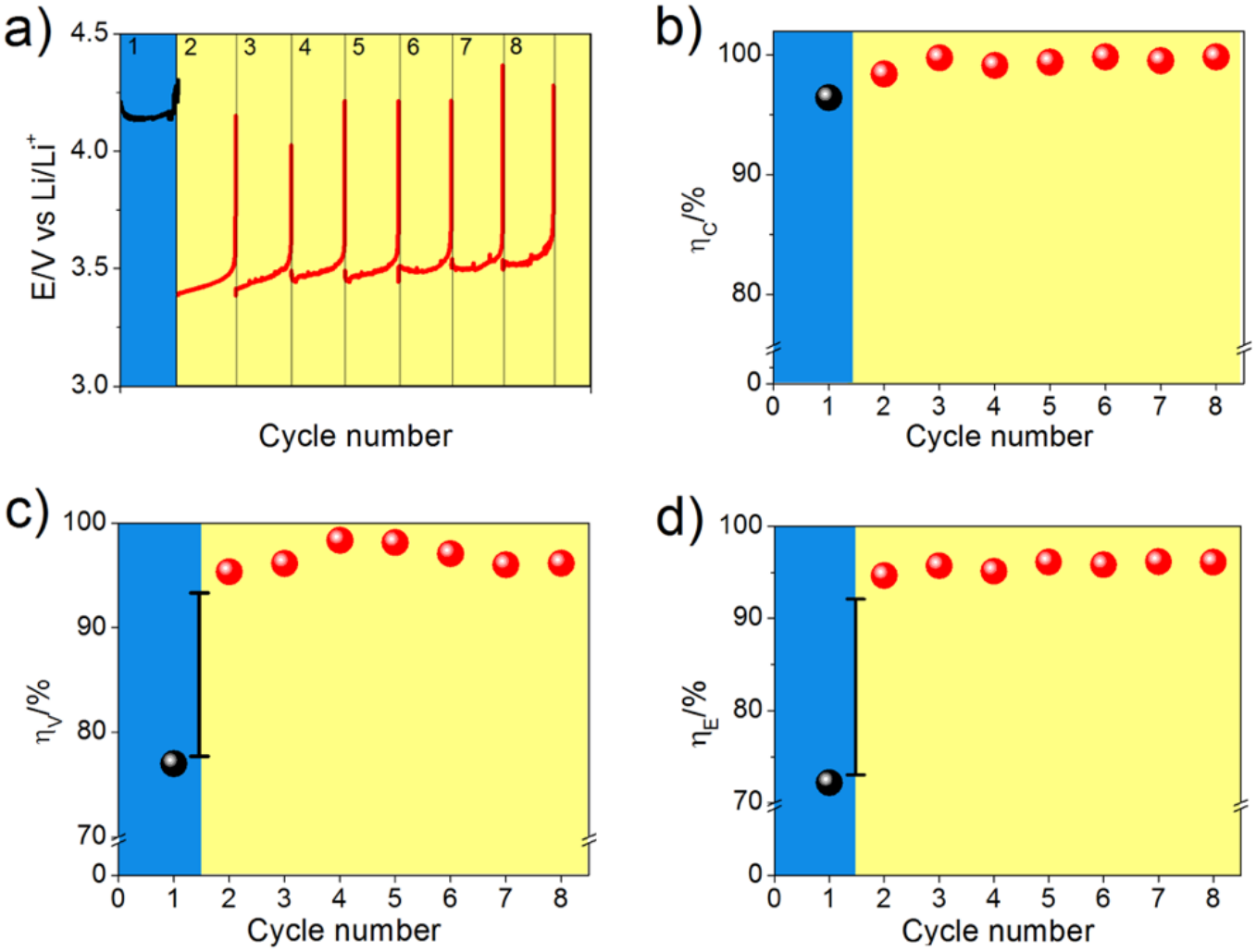

The illumination improves energy efficiencies > 20%.

Technical Challenges

- **Stability**
  - The most photochemically stable semiconductors in aqueous solution are oxides, but their band gaps are either too large for efficient light absorption (~3 eV), or their semiconductor characteristics are poor.
- **Efficiency (Bandgap)**
  - For reasonable solar efficiencies, the band gap must be less than 2.2 eV, unfortunately, most useful semiconductors with bandgaps in this range are photochemically unstable in water.
- **Energetics**
  - In contrast to metal electrodes, semiconductor electrodes in contact with liquid electrolytes have fixed energies where the charge carriers enter the solution. So even though a semiconductor electrode may generate sufficient energy to effect an electrochemical reaction, the energetic position of the band edges may prevent it from doing so. For spontaneous water splitting, the oxygen and hydrogen reactions must lie between the valence and conduction band edges, and this is almost never the case.